# Regional differences in soil stable isotopes and vibrational features at depth in three California Grasslands

**Authors: L.M. Wahab[1], S.S. Chacon[1], S.L. Kim[1], A.A. Berhe[1]**

[1]Life and Environmental Sciences Department, University of California – Merced

Corresponding author: Leila Maria Wahab (lwahab@ucmerced.edu)

**ORCiD:**

L.M. Wahab: 0000-0002-9997-1987

S.L Kim: 0000-0002-4900-3101

S.S Chacon: 0000-0001-7599-9152

A.A. Berhe: 0000-0002-6986-7943

This paper is a non-peer reviewed pre-print submitted to EarthArXiv. This manuscript was submitted to Springer Biogeochemistry for peer review.

**Abstract**

There are major gaps in our understanding of how Mediterranean ecosystems will respond to anticipated changes in precipitation. In particular, limited data exists on the response of deep soil carbon dynamics to changes in climate. In this study we wanted to examine carbon and nitrogen dynamics between topsoils and subsoils along a precipitation gradient of California grasslands. We focused on organic matter composition across three California grassland sites, from a dry and hot regime (~300 mm precipitation; MAT: 14.6℃) to a wet, cool regime (~2160 mm precipitation/year; MAT: 11.7℃). We determined changes in total elemental concentrations of soil carbon and nitrogen, stable isotope composition ($\delta^{13}C$, $\delta^{15}N$), and composition of soil organic matter (SOM) as measured through Diffuse Reflectance Infrared Fourier Transformed Spectroscopy (DRIFTS) to 1m soil depth. We measured carbon persistence in soil organic matter (SOM) based on beta ($\boldsymbol{\beta}$), a parameter based on the slope of carbon isotope composition across depth and proxy for turnover. Further, we examined the relationship between $\delta^{15}N$ and C:N values to infer SOM's degree of microbial processing. As expected, we measured the greatest carbon stock at the surface of our wettest site, but carbon stocks in subsoils converged at the wet and dry sites. Soils at depth (>30cm) at the wettest site had the lowest C:N and highest $\delta^{15}N$ values with the greatest proportion of simple plant-derived organic matter according to DRIFTS. These results suggest differing stabilization mechanisms of organic matter at depth across our study sites. We infer that the greatest stability was conferred by associations with reactive minerals at depth in our wettest site. In contrast, organic matter at our driest site was subject to the most microbial processing. Results from this study demonstrate that precipitation patterns have important implications for deep soil carbon storage and composition, suggesting vulnerability of deep SOM to climate change induced alterations in precipitation patterns.

Key words: Biogeochemical Cycles, Soil Carbon, Precipitation, Grasslands

## 1 Introduction

Grasslands account for 34% of the terrestrial carbon stock and are susceptible to global changes in precipitation and temperature patterns over the coming centuries (Bai & Cotrufo, 2022). In California, grasslands account for 15% of the land area, with native intact grasslands being one of the state's most threatened ecosystems (D'Antonio et al., 2002). Climate change is predicted to intensify the hydrologic cycle and increase temperatures globally (IPCC, 2022). Shifts in the amount and timing of precipitation can potentially lead to loss of carbon stocks within grasslands since key biogeochemical processes, plant communities, and fungal communities are sensitive to environmental conditions (Chou et al., 2008; Deepika & Kothamasi, 2015; Fay et al., 2002; Knapp, 2002; Suttle et al., 2007). Plant community composition and diversity, especially in Mediterranean grasslands, are sensitive to shifts

in precipitation patterns (Suttle et al., 2007; Suttle & Thomsen, 2007). Further, increasing temperature is shown to decrease soil organic carbon (SOC) stock in grasslands through feedbacks with carbon degrading enzymes, such as ligninase and cellulase activity (Chen et al., 2020). However, elevated $pCO_2$ is suggested to increase SOC stock in grasslands by triggering greater carbon allocation belowground (Terrer et al., 2021). This picture of changing SOC dynamics under climate change is further complicated once we integrate depth, leading to uncertainty regarding grassland carbon sequestration potential (Bai & Cotrufo, 2022).

Subsoils (>30cm) store the majority of the of the global soil carbon pool (Jobbágy & Jackson, 2000), but current measurements in the field of SOC and SOM stability are largely limited to topsoil (<30cm) (Yost & Hartemink, 2020). The bias of current studies towards topsoil is typically due to greater access and abundance of organic matter and biomass in topsoils. However, more focus on subsoil SOM dynamics is warranted since subsoils are better suited to long-term carbon sequestration (Button et al., 2022) Physical, chemical, and biological factors important for understanding SOC stocks and stability vary between topsoils and subsoils, though to differing degrees depending on soil order (Button et al., 2022; Hicks Pries et al., 2023). These factors can include bulk density, pH, and Fe/Al oxide concentration, and are essential for understanding stabilization mechanisms and residence times of SOM across depths (Button et al., 2022). Under most conditions, SOM persistence tends to be greater in subsoils, as indicated by longer residence times based on radiocarbon measurements (Rumpel, 2004). However, limited data exists on SOM persistence in subsoils for soils across precipitation gradients. In this study, we define stability as the likelihood of organic matter to persist in soil rather than being decomposed, leached, eroded, and eventually respired as $CO_2$. Occlusion and mineral association act as physical and chemical mechanisms of stability, respectively, decreasing the likelihood of SOM being decomposed. A caveat is that roots can impact the protective effects of occlusion and mineral association within the rhizosphere (Jilling et al., 2018; Schmidt et al., 2011). Field studies have the added benefit of providing realistic plant input and environmental fluctuation of subsoil carbon dynamics that are clearly needed for a better understanding of their sequestration potential under climate change as well as for their integration into models of SOM dynamics under changing environmental conditions.

Stable isotope composition, such as $\delta^{13}C$ and $\delta^{15}N$ can be informative in disentangling complex subsoil depth patterns. The natural abundance of carbon and nitrogen isotopes, specifically $^{13}C$ and $^{15}N$, can be informative for several ecologically relevant processes on decadal and centennial timescales. For example, the vertical distribution of $\delta^{13}C$ values in soil profiles can be used to understand the balance between C3 and C4 grasses in an ecosystem, SOC

processing, and microbial activity (Ehleringer et al., 2000; Staddon, 2004; Wang et al., 2018). C3 plants in particular have a well-documented physiological response to increasing aridity that leads to high $\delta^{13}C$ values (Farquhar et al., 1989; Hartman & Danin, 2010; Kohn, 2010). This interaction between precipitation and the stable isotope content of plant matter means that the inputs for formed C will be affected by climate. The $\delta^{15}N$ values have also been shown to increase in arid environments, though the direct mechanism is less clear (Aranibar et al., 2004; Craine et al., 2015). Nitrogen inputs can occur through both atmospheric deposition and biological $N_2$ fixation. Inputs from biological fixation produce $\delta^{15}N$ values close to 0‰ (Högberg, 1997; Robinson, 2001), while per mille values from N deposition can have a wide range. Constraining the range of isotopic values for N deposition inputs are current areas of study due to increased nitrogen loading in ecosystems over time (Agnihotri et al., 2011; Chen, et al., 2020). However, the vertical distribution of $\delta^{15}N$ values is a useful proxy for SOM processing, and the balance between abiotic and biotic drivers of the nitrogen cycle (Conen et al., 2013; Hobbie & Ouimette, 2009a). The depth trends of $\delta^{13}C$ in bulk soil tend to be related to the shift in microbial contributions and plant components, rather than microbial fractionation during decomposition (Ehleringer et al., 2000), tracking changing inputs of fungal and microbial biomass with depth (Kohl et al., 2015). Disentangling the many interacting processes related to carbon and nitrogen cycling can be difficult because it can often mean detecting small changes in a large pool. However, integrative approaches using stable isotopes can be uniquely useful in quantifying and comparing ecosystem processes.

Relationships between C:N and $\delta^{15}N$ are linked to the processing and persistence of SOC and can be a useful proxy for disentangling depth patterns (Brunn et al., 2014; Conen et al., 2008, 2013). The transition from particulate organic matter (POM) to mineral-associated organic matter (MAOM) results in an inverse relationship. For example, low $\delta^{15}N$ value and high C:N can indicate POM, whereas higher $\delta^{15}N$ values and low C:N indicate MAOM, or greater stability (Conen et al., 2008). There is greater complexity underlying this continuum between POM and MAOM, and MAOM does not always correlate with greater stability and persistence (Sokol et al., 2022). However, the inverse relationship between the $\delta^{15}N$ and C:N indicates nitrogen loss in ecosystems; "leaky" systems are indicated by higher C:N and $\delta^{15}N$ values as $^{14}N$ is lost during volatilization or denitrification (Conen et al., 2013). Isotope values and elemental concentrations can also discern nutrient turnover pools with indicators of SOM stability, such as $\beta$, the slope of $\delta^{13}C$ ,and log-transformed carbon concentration has good agreement with SOC turnover calculated from steady-state equations (Garten, 2006). Previous studies indicate similar turnover results estimated using $\beta$ and existing

methods, such as radiocarbon age, and have related it to climatic factors, such as soil water conditions (Acton et al., 2013; Garten, 2006) in global datasets (Wang et al., 2018) and chronosequences (Brunn et al., 2016). Overall, the natural abundance of stable isotopes provides valuable ecological information and enhance our ability to understand soil processes at a variety of depths and ecosystems, especially when paired with elemental carbon and nitrogen data and spectroscopic data.

In our study, we conducted soil measurements to 1m depth across three California grasslands that exist along a climatic gradient to compare topsoil and subsoil SOM dynamics in three different climatic regimes (see the edaphic characteristics of each site in Table 1). A recent study at these sites showed that the climate gradient strongly influenced growing soil microbial communities and turnover rates based on soil $\Delta^{14}C$ (Foley et al., 2023); our study complements this dataset by examining stable isotopes and functional group chemistry to depth (1m) at the same locations. We investigated the natural abundance of $^{13}C$ and $^{15}N$, and isotopic proxies of stability and turnover in combination with Diffuse Reflectance Fourier Transform Spectroscopy (DRIFTS) to study the impact of both climatic factors and depth on soil carbon and nitrogen content and processes. Our study sought to answer three critical questions: 1) Are there variations in carbon concentration and stock between topsoil and subsoil across precipitation and temperature gradients? We hypothesized that soils in wetter climates would accrue more carbon in deeper soil layers due to high plant productivity and favorable mineralogy to retain carbon in deeper soils. 2) Are there differences in depth distributions of $\delta^{13}C$ and $\delta^{15}N$ stable isotopic signatures with varying climate? Additionally, do turnover and transformation of organic matter vary between topsoil and subsoil across precipitation and temperature gradients? Isotopic values were hypothesized to be increased at in topsoils at our drier site. We also hypothesized that isotope values would be increased in subsoils at our wetter site, and would reflect a greater microbial signature. 3) Does the functional group chemistry of SOM vary across precipitation and temperature gradients and along depth profiles? Finally, regarding functional group chemistry, we hypothesized that there would be greater simple plant matter remaining in the profile at the driest site. We also hypothesized that there would be a greater proportion of microbially processed organic matter at the wettest site.

## 2 Materials and Methods

### 2.1 Study Area

Soil samples were collected at three annual grasslands: Sedgwick National Reserve (Suttle et al., 2007), University of California Hopland Research and Extension Center and the Angelo Coast Range Reserve in California (fig.1). Each site is an established reserve site within the University of California system, and, as such, has detailed information on vegetation and climatic factors. All three sites have not been exposed to agriculture, and do not have a history of C4 plants being present but are dominated by exotic annual grasses, while forbs are of both native and exotic origin. The dominant vegetation at Angelo is *Aira* spp., *Bromus* spp, and *Briza* spp. (Foley et al., 2023). At Hopland, it is a mix of *Avena* spp., *Bromus* spp., *Erodium* spp., and *Festuca* spp. (Foley et al., 2023). At Sedgwick, the dominant vegetation is *Avena* spp. and *Bromus* spp. (Foley et al., 2023). To further assess differences in plant communities, we aggregated all citations associated with plant surveys at each of our study sites (Supplemental Table 1). We then further aggregated information about whether each species was C3/C4, native/introduced, or is a N-fixing or non-N-fixing plant. This helped us determine potential plant community impacts on isotopic values. Plant communities in this region are typically dominated by C3 annual grasses.

All soils across these sites have a xeric soil moisture regime (xer-), which indicates Mediterranean climates with wet, cool winters and warm, dry summers. At Angelo, soils are mapped as part of the Holohan-Hollowtree-Casabonne Complex, formed largely in gray wacke and mudstone. These are Alfisols with argillic (clay-enriched) or kandic (highly weather clay) subsoil horizons (Ultic Haploxeralfs). At Hopland, soils were largely formed from sandstone and shale and are part of the Yorkville soil series; these are Mollisols with argillic subsoil horizons (Typic Argixerolls). Soils at Sedgwick have been mapped as the Salinas soil series: Mollisols with the presence of calcium carbonate in subsoil horizons (Pachic Haploxerolls). Parent material is sandstone and shale at Sedgwick. There has been substantial discussion regarding the contributions of petrogenic carbon to soils from shale parent materials (Grant et al., 2023), which has been observed at Sedgwick (Bingham et al., 2021). Bingham et al. (2021) showed evidence of rock-derived nitrogen at depths greater than 1m in Sedgwick soils, and saw increased $\delta^{15}N$ values (~6‰) associated with these inputs.

### 2.2 Experimental Design and Sampling

Soils were collected to 1m across the three study sites, Angelo, Hopland, and Sedgwick. Samples at Hopland and Sedgwick were collected by hand auger to 1m with 6-7 replicates per site, each site encompassing approximately 3 ha. We attempted to capture spatial heterogeneity but avoid confounding factors at each site by evenly sampling across similar slope positions (only Hopland had significant relief). At Angelo, samples were collected by Geoprobe due to being part of a different sampling campaign and were collected to depth of resistance (approximately 3m) with 4 replicates. Depths greater than 1m are not reported for Angelo in this study. At all sites, samples were collected at consistent 10cm intervals (0-10, 10-20, and so on).

After collecting soils, transported in coolers with ice packs and stored in a 4℃ cold room for approximately 4 months until they could be subsampled and analyzed. Long storage times occurred due to a lack of access to laboratory facilities due to the COVID-19 pandemic and subsequent shutdown procedures When laboratories were opened and samples could be processed, a subsample was removed from each sample, and air dried for 7 days at room temperature. Soil samples were tested for carbonates by observing the presence and degree of effervescence with a few drops of 1 M Hydrochloric acid. Following air drying, the sample was then processed through a 2mm sieve and a subsample was used for ball milling (using a Sample Prep 8000M Ball Mill) to a homogenous particle size. These homogenized samples were used for stable isotope at DRIFTS analysis.

We collected bulk density at Angelo and Hopland through Geoprobe cores, and calculated carbon stocks with these bulk density estimates. At Angelo, we subsampled each depth increment to estimate water content, and then calculated the dry mass of soil in a 10cm increment. Bulk density was calculated as the mass of the dry >2mm fraction to correct for the impact of rock and root volume on soil carbon and nitrogen stocks (Throop et al., 2012). We did not observe a high contribution of coarse fraction at Hopland. At Sedgwick, due to difficulties with collecting bulk density cores at depth in an arid environment, we used a pedotransfer function to calculate bulk densities at this site. We used a pedotransfer function calibrated for Californian soils (Alexander, 1980) that was recently evaluated to accurately estimate of bulk density (Abdelbaki, 2018). The equation we used from Alexander (1980) to derive an estimate of bulk density at Sedgwick:

$$Bulk\ density\ (\frac{g}{cm^3}) = 1.66 - 0.308\ (OC)^{0.5} \qquad \text{Equation 1}$$

This equation was recently evaluated to accurately estimate bulk density (Abdelbaki, 2018). We further compared the results of this bulk density pedotransfer function on the estimated versus measured carbon stocks at Angelo and Hopland (fig. S1).

### 2.3 Elemental and Isotopic Analyses

Elemental and isotopic composition of carbon and nitrogen (i.e., %C, %N, $\delta^{13}C$, $\delta^{15}N$ values) in in all samples were measured in the Stable Isotope Ecosystem Laboratory at the University of California, Merced (SIELO). Briefly, samples were weighed into tin capsules and combusted in a Costech 4010 Elemental Analyzer coupled with a Delta V Plus Continuous Flow Isotope Ratio Mass Spectrometer. Carbon and nitrogen isotope compositions were corrected for instrumental drift, mass linearity, and standardized to the international VPDB ($\delta^{13}C$) and AIR ($\delta^{15}N$) scales using the USGS 41A and USGS 40 standard reference materials. Mean $\delta^{13}C$ values for reference materials were USGS 40 = -26.4 ± 0.1‰ (n = 173) and USGS 41a = 36.5 ±0.2‰ (n = 87) and corresponding mean $\delta^{15}N$ values were USGS 40 -4.5 ± 0.1‰ (n = 173) and USGS 41a 47.5 ± 0.1‰ (n = 87). Elemental carbon and nitrogen content were determined via linear regression of $CO_2$ and $N_2$ sample gas peak areas against the known carbon and nitrogen contents of USGS 40, USGS 41a, and Costech acetanilide. All isotope compositions are expressed in standard delta notations.

### 2.4 Diffuse Reflectance Infrared Fourier transform Spectroscopy (DRIFTS)

To characterize the chemical composition of soil C across our study systems, we used Diffuse Reflectance mid-Infrared Fourier Transform spectroscopy (DRIFTS) analyses on bulk soil samples. DRIFTS measures the vibrational frequencies of functional groups found in soil organic matter and mineral surfaces. In addition, DRIFTS is informative on the abundance of organic and inorganic substances by measuring the excitation of molecular bonds when exposed to infrared radiation (Parikh et al., 2014). We used a Bruker IFS 66v/S Spectrophotometer (Ettlingen, Germany) with a praying Mantis apparatus (Harrick Scientific, Ossining, NY) at the Nuclear Magnetic Resonance (NMR) lab at UC Merced. Potassium bromide (KBr) was used as a background reference, but samples were not diluted with KBr. Samples were first dried in a desiccator following homogenization to remove interference from water. Absorption was measured between 4000 and 400 $cm^{-1}$ averaged over 300 scans with an aperture of 4mm. Functional groups for simple plant carbon (aliphatic C-H; λ: 2976-2898 $cm^{-}$), complex plant carbon (aromatic C=C; λ: 1550-1500 $cm^{-1}$), microbially derived carbon (amide/quinone/ketone, CO; aromatic, CC, carboxylate COO; λ: 1660-1580 $cm^{-1}$) were assigned following Mainka et al. (2022), also shown in Table 2 (Mainka et al., 2021; Parikh et al., 2014; Vranova et al., 2013). Microbial derived carbon more specifically originate from microbial cell wall

constituents (Mainka et al., 2021). Wavenumbers that overlap with signals from mineral compounds (i.e., 1400-400 $cm^{-1}$), were excluded from the analysis (Margenot et al., 2015; Parikh et al., 2014). We also calculated ratios of simple plant carbon to microbial carbon, as well as complex plant carbon to microbial carbon. These ratios are helpful indicators of proportional contribution and biological processes; and a low ratio of simple plant carbon to microbial carbon indicates microbial oxidation of plant derived carbon and a high ratio of complex plant carbon to microbial carbon indicates a high supply of aromatic plant compounds to soil (Figure 1e).

### 2.5 Satellite-based remote sensing imager and processing MODIS imagery to calculate Normalized Difference Vegetation Index

Normalized Difference Vegetation Index (NDVI) is used to quantify vegetation greenness, and is used as a proxy for plant productivity. The NDVI ratio is an indicator of vegetation greenness, and a greater NDVI value indicates more greenness or greater plant productivity. We downloaded the Terra/MODIS surface reflectance (MOD09Q1.5) 8-day L3 global 250-m product from NASA's Earth Science Data System (https://www.earthdata.nasa.gov/) for the year 2020 (the same year sites were sampled) at all three sites in this study. This reflectance product provides a measure of surface reflectance at the ground level, and data were projected in a MODIS specific sinusoidal projection. These eight-day composite images represent the maximum surface reflectance over that time period while minimizing atmospheric effects, like clouds and aerosols. We used band 1 (620-670 nm) and band 2 (841-876 mm) to calculate NDVI over the entire MODIS image using the following equation:

$$NDVI = \frac{band\ 2 - band\ 1}{band\ 2 + band\ 1} \qquad \text{Equation 2}$$

Afterward, we plotted data over the year 2020 (fig. S2) and computed the average value over the entire year (table 1).

### 2.6 Statistical Methods, calculation of turnover index ($\beta$ values), and processing index

Differences between sites were evaluated through a combination of one-way ANOVA and Tukey's HSD within each 10cm depth interval. Statistical significance was evaluated using $\alpha = 0.05$. All statistical analyses were performed in R.

The response of $\delta^{13}C$ values to SOC on logarithmic scale is termed $\beta$ and is associated with isotopic fractionation due to decomposition and physical mixing (Acton et al., 2013). Using $\delta^{13}C$ values represents a natural (unlabeled) and high throughput methodology for measuring carbon accumulation and turnover dynamics across

varied ecosystems (Acton et al., 2013). $\beta$ is comparable to established techniques for measuring turnover, like radiocarbon measurements. $\beta$ values indicate the rate that SOC $\delta^{13}C$ values vary with depth (Acton et al., 2013; Garten, 2006; Garten & Hanson, 2006) and change based on environmental factors, such as soil texture and soil water conditions (Campbell et al., 2009).The $\beta$ values were derived from the slopes of linear regressions between log transformed C contents (log (C%)) and their respective $\delta^{13}C$ values (‰ VPDB). In this case, the $\beta$ values can be interpreted as the change in $\delta^{13}C$ for every 10-fold increase in SOC content, and is indicative of isotopic fractionation during decomposition and recycling of SOC from fresh litter to more processed (Acton et al., 2013; Brunn et al., 2014; Garten & Hanson, 2006). In this study, we interpreted steeper slopes, or greater $\beta$ values, as greater turnover through decomposition or physical mixing, as it is indicative of processed litter.

A complementary indicator to soil turnover (beta) is relating C:N (calculated on a weight basis) and $\delta^{15}N$ values to evaluate organic matter processing. Previous studies show this relationship is strongly tied to POM and MAOM in soils (Brunn et al., 2014; Conen et al., 2008, 2013) and indicates material that has undergone a greater degree of microbial processing. Here, we interpret high $\delta^{15}N$ and low C:N values as indicative of more processed soil carbon, and low $\delta^{15}N$ and high C:N as less processed soil carbon. However, other studies have found in systems with substantial short range order oxide concentrations to have low C:N and low $\delta^{15}N$ in the densest and most stable fractions (Sollins et al., 2006, 2009).

We consider both the proxy $\beta$ and the relationship between C:N and $\delta^{15}N$ values to be complementary indices for soil turnover, rates of decomposition, and physical/chemical protection of soil carbon. More specifically, we interpreted $\beta$ (hereafter termed our turnover index) as processing due to decomposition and mixing, whereas the relationship between $\delta^{15}N$ and C:N (hereafter termed our processing index) is related to physical and/or chemical protection of soil carbon and decomposition through microbial metabolism.

## 3 Results

### 3.1 Elemental data across the precipitation gradient of ecosystems

When evaluating concentrations of carbon and nitrogen in soil at each of the sites, we observed important differences in C:N ratios across the three sites. We determined that total carbon = organic carbon in all our sites as testing with 1.0 M Hydrochloric acid resulted in no effervescence, indicating that the contribution of carbonates to

total organic carbon was minimal even in soils mapped as the Salina soil series in Sedgwick. In topsoils (0-30cm), we didn't detect significant differences in carbon and nitrogen abundance between sites. However, carbon concentrations started to differ at 40 cm depth ($p<0.05$) (fig. 3a). The largest difference in subsoils carbon and nitrogen concentrations, and hence C:N ratio was observed between our wet and dry sites, Angelo and Sedgwick, respectively, especially at 40 cm and, between 60 and 90cm ($p<0.05$). Nitrogen abundance was similar between all sites (fig. 3b), and converged to similar nitrogen concentrations from 15 cm to 75 cm (~0.06%). We observed C:N values ranging from 10-12 at Hopland and Sedgwick for most of the depth profile. At Angelo, lower C:N values were detected for the majority of its profile (fig. 3c), which was significantly different from the other sites ($p<0.0001$) and persisted throughout the depth profile (50-90 cm). Carbon stocks were significantly higher at Angelo and Hopland in topsoils (fig. 4). In subsoils, however, Sedgwick and Angelo had relatively similar carbon stocks. Hopland had the greatest subsoil carbon stocks. Overall, differences between sites were related to C:N ratios, largely driven by low carbon concentrations and stocks at depth at Angelo (the wettest site).

### 3.2 Isotopic data across the precipitation gradient of ecosystems

All sites had similar $\delta^{13}C$ values at the surface but differences emerged at 20 cm and continued until 50 cm between Angelo and Hopland (fig. 3d). Angelo had the greatest values between 30-70 cm (-25±0.2‰) and Hopland had the lowest values (-27 ± 0.1‰) within this depth profile (fig. 3d). At 60cm, we observed differences in $\delta^{13}C$ values between all sites ($p<0.0001$). However, nitrogen isotope patterns were more consistent within sites and there were no clear differences between topsoils and subsoils. Overall, Hopland had the greatest $\delta^{15}N$ values (3.7 ± 0.3‰), Sedgwick (2.7 ± 0.2‰) had intermediate values, and Angelo had the lowest values (1.8 ± 0.1‰) (fig. 2e). Hopland differed significantly in $\delta^{15}N$ value from both Angelo and Sedgwick at 10cm, an effect that persisted to 30cm ($p<0.0001$). Although the $\delta^{15}N$ values at Hopland were initially greater than Sedgwick, at 50cm this pattern switched and Sedgwick $\delta^{15}N$ values at depth were greater than Angelo for the deeper depths (fig. 3e). However, there were no statistical differences among sites in $\delta^{15}N$ between 50-90cm. Sites did differ significantly in $\delta^{15}N$ values at 100cm ($p<0.05$). Overall, we observed the greatest differences in isotope composition in the $\delta^{13}C$ values between sites, and between topsoils and subsoils, suggesting complex and interactive effects of climate with carbon cycling at depth.

### 3.3 Indices of turnover and proccessing and correlations with depth

Processing and turnover proxies were based on elemental and isotopic compositions at each site and across depth profiles. The turnover index, $\beta$, used elemental and isotopic data to discern the rate of change in $\delta^{13}C$ values with log-transformed C concentration. All localities in this study had different and negative $\beta$ values (fig. 5). Sedgwick, the warmest and driest site (MAT: 14.6℃; MAP: ~300 mm precipitation/year), had the greatest β value of -1.8 ($R^2$ = 0.89, $p$ < 0.001) followed by Angelo, the coolest and wettest site (MAT: 11.7℃; MAP: ~2160 mm precipitation/year) with β value of -1.2 ($R^2$ = 0.93, $p$ < 0.001). Hopland with intermediate temperature and precipitation (MAT: X; MAP: Y) had the lowest β value of -0.70 and best fit ($R^2$= 0.94, $p$ < 0.001) (fig. 5). Overall, the turnover index, β, was the greatest at our driest and warmest site and lowest at our intermediate site.

In contrast to the turnover index, the index used to discern SOM processing was based on $\delta^{15}N$ values versus C:N ratios, which highlighted unique relationships per field site (fig. 6a-c). At Angelo, surface samples (from 0-30 cm) had high C:N (8-10) and $\delta^{15}N$ values (fig. 6a) while samples at depth (>30cm) had much lower C:N values (~4-5) (fig. 6a). At Hopland and Sedgwick, we did not observe a strong separation by depth category for C:N or $\delta^{15}N$ values (fig. 6b-4c). Specifically at Hopland, surface samples and samples at depth separated more weakly by C:N values (fig. 6b), while at Sedgwick, all samples at all depths clustered around similar C:N values, and there was no consistent variation of depth with either C:N or $\delta^{15}N$ values (fig. 6c). Strikingly, Angelo was the only site with strong depth separation for our processing indicator.

### 3.4 Predominant chemical moieties of organic carbon shifts across sites and depth

DRIFTS indicates functional group differences of organic matter across sites (fig. 7). The proportion of functional groups categorized as simple plant-derived OM was generally higher in Angelo soils than at Sedgwick and Hopland, with significantly higher proportions detected below 60 cm depths (fig 8a, $p$<0.05). Significant differences in the complex plant-derived OM were not detected above 30 cm across all sites; significant shifts occurred for complex plant C below 50 cm (fig 8b, $p$<0.05). Hopland soils had significantly higher proportions of complex plant-derived OM at 70 and 90 cm depths than Angelo and Sedgwick soils ($p$<0.05); meanwhile, Angelo soils showed significant decreases starting at 60 cm ($p$<0.05). The proportion of microbially derived OM was significantly lower across all depths in Angelo soils when compared to the other sites (fig 8d, $p$<0.05). No significant differences in microbially derived OM were detected between Sedgwick and Hopland soils throughout the entire soil profile. The combination of lower proportion of microbially associated OM and higher proportion of simple plant-derived

compounds at Angelo resulted in a greater simple plant matter to microbially associated OM ratio (fig. 8d, $p<0.05$). Sites all had a similar complex plant matter to microbial OM ratio, and there were almost no statistically significant differences except at 40cm (fig. 8e).

### 3.5 Differences in plant productivity across the gradient as indicated by NDVI

NDVI was greatest at the wettest site, Angelo, and similar between Hopland and Sedgwick (Table 1). We also observed seasonal variability in NDVI at Hopland and Sedgwick, with the greatest NDVI occurring in the spring months (Mar-Apr) and decreasing from the summer to winter (Jun-Dec) (fig. S2). Angelo had a consistently high (~0.9) NDVI throughout the year (fig. S2).

## 4 Discussion

Elemental data from our sites, including carbon and nitrogen concentrations, C:N ratios, and carbon stocks indicated differences balance of carbon inputs and outputs at each site, providing clues for difference in mechanisms of SOM stabilization across our sites. The wettest site, Angelo, had the greatest surface carbon stocks but also the greatest proportion of simple plant-derived OM in subsoils. Our intermediate site, Hopland, had visual evidence of redox sites, and these were also indicated by greater heterogeneity in functional groups present and low $\delta^{13}C$ values. And finally, our driest site, Sedgwick, had the highest turnover and least differentiation between topsoils versus subsoils based on our processing indicator. Our results highlight the importance of considering regional differences in processing and turnover of subsoils for carbon sequestration efforts.

### 4.1 Elemental variations indicate different inputs to stable carbon pools

The greatest elemental variations were between C:N values and carbon stocks between sites. We observed the greatest carbon concentration across the depth profile at Sedgwick, the driest locality of our three sites (MAP: 24mm/year; fig. 3a) whereas the wettest site Angelo (MAP: 126 mm/year), had the lowest C:N values, especially at depth. We hypothesized the wettest sites would have the greatest carbon and nitrogen concentrations due to greater biomass input (Aranibar et al., 2004), which would also result in higher C:N; however our results did not conform to this simplistic schema. We observed greater plant inputs at Angelo through NDVI (table 1) and greater surface stocks from our results, but subsoil carbon stocks were relatively similar between our wettest and driest site (fig. 4). The slightly greater carbon accrual in subsoils at Sedgwick is consistent with conclusions of recent studies that dry conditions lead to lower decomposition rates (Berthrong et al., 2012; Campo & Merino, 2016; Chai et al., 2022;

Fröberg et al., 2008; Heckman et al., 2023; Zhang et al., 2015), but carbon accrual in dry conditions would be expected to be dampened by decreasing plant litter inputs. However, we observed relatively similar subsoil carbon stocks between Angelo and Sedgwick (fig. 4). In a recent meta-analysis, decreased precipitation slowed carbon cycling processes across a wide gradient of ecosystems; semi-arid and temperate grasslands were particularly sensitive to increased precipitation (Song et al., 2019). Furthermore, there is evidence from manipulation studies that increased precipitation affects ecosystem carbon balance in grasslands due to increases in soil respiration (Chou et al., 2008; Harper et al., 2005). This interaction between precipitation and carbon balance is further complicated by carbon stock trends with depth at our sites. We observed the greatest carbon stocks in topsoils (0-30cm) at the wet and intermediate site. However, we noted that the wet and dry sites approached similar carbon stock values deeper in the subsoils profile (below 30 cm); in contrast, our intermediate site actually had the greatest carbon stock in subsoils below 30 cm (fig.4). The effects of changing climatic dynamics are further complicated by including the effects of warming, which has been shown to decrease POM (Rocci et al., 2021) and enhance the formation of newly synthesized carbon in subsoils (Jia et al., 2019). Overall, we observed key differences in C:N value and carbon stocks between topsoils and subsoils across ecosystems.

While carbon signals across sites clearly differed, it is crucial to consider carbon and nitrogen together due to the impact of nitrogen limitation in modulating plant and microbial activity. There is evidence of asymmetric responses to climatic regime changes that could affect soil carbon and nitrogen composition and/or cycling. For example, a precipitation manipulation study in a shortgrass steppe ecosystem found that long term drought significantly reduced $CO_2$ flux and caused accumulation of inorganic nitrogen (Evans & Burke, 2013). This previous study suggests a decoupling of carbon and nitrogen cycling resulting in the observation that nitrogen mineralization and decomposition may have different sensitivities to moisture (Evans & Burke, 2013). In addition, field experiments in agricultural grassland ecosystems indicate decoupled carbon and nitrogen persistence as mineral associated carbon in necromass declines more rapidly than nitrogen (Buckeridge et al., 2022). This is likely occurring at Angelo, as indicated by low C:N at depth (fig. 3c) and differing functional group character as indicated by high proportions of simple plant-derived OM throughout the profile (fig. 3d).

Historical, elemental, and functional group data in subsoils allowed us to make some inferences regarding stabilization mechanisms for carbon in these ecosystems. We hypothesized that we would see the greatest persistence of simple plant matter at the driest site, and greater evidence for microbial oxidation at the wettest site. However, the

greatest ratio of simple to microbially associated OM was in Angelo subsoils (fig. 3e) while the ratio of complex to microbial associated OM was similar across all sites. We expected greater microbial oxidation at our wettest site, but instead DRIFTS results provided the greatest evidence of this at our dry and intermediate site through DRIFTS. Overall, there was greater persistence of plant inputs throughout the profile at Angelo (Fig. 8a). Soils at Angelo are rich in Fe/Al short range order mineral surfaces (SRO) (Berhe et al., 2012) while soils at Sedgwick have no measurable Al minerals (Foley et al., 2023). Soils at Sedgwick also have the greatest surface clay content (Table 1) and a greater base cation concentration (Foley et al., 2023). These base cations serve as a key stabilization mechanism due to cation bridging between OM and mineral surfaces (Aquino et al., 2011). Our results suggest greater persistence of microbial byproducts and plant inputs at Angelo, which could be contributing to mineral associated organic matter (MAOM) at depth. Whereas at Sedgwick, stabilization is likely driven by clay content and greater base cation concentrations that facilitate MAOM formation through cation bridging. We also saw greater evidence of microbial oxidation at depth in Sedgwick with DRIFTs, which is consistent with its high turnover index value derived from stable isotopes and concentration.

Spectral features from DRIFTS data and low C:N values are indicative of greater persistence of plant and microbial carbon in subsoils at Angelo. We detected low C:N (<5) values at Angelo compared to Sedgwick and Hopland (fig. 3c). The C:N ratios of SOC can be influenced by the catabolic and anabolic metabolisms of soil microbes. The production and recycling of metabolites and the generation of biomass lower the C:N ratios of SOC while fresh plant inputs can increase the C:N ratios. Thus, the low C:N values measured at depth in the soils at Angelo could be caused by greater microbial processing of SOC and necromass at depth in Angelo soils. In fact, necromass has been shown to be a significant portion of SOC in grasslands (Buckeridge et al., 2020, 2022; Liang et al., 2019; B. Wang et al., 2021). Our elemental, isotopic, and spectroscopic measurements were all done on bulk soils, so we are likely observing a combination of inactive microbial biomass, necromass, and plant inputs.

### 4.2 Variance of $\delta^{13}C$ and $\delta^{15}N$ values explained by depth and biotic factors

We observed a strong depth correlation with $\delta^{13}C$ values, but not $\delta^{15}N$ values across the three sampled localities. We hypothesized that $\delta^{13}C$ and $\delta^{15}N$ values would be greatest at our most arid site. However, $\delta^{13}C$ and $\delta^{15}N$ was relatively similar between Angelo and Sedgwick. Sedgwick subsoils had the greatest $\delta^{15}N$ values in subsoils at Sedgwick, which could be influenced by rock derived and inorganic nitrogen (Bingham et al., 2021). While

409 photosynthetic pathways are a key influence on surface $\delta^{13}C$ values, all sites were similarly dominated by C3
410 vegetation and therefore exhibited similar surface $\delta^{13}C$ values (table S1). Furthermore, introduced annual grasses with
411 shallow roots dominated our sites (table S1). In general, $\delta^{13}C$ values increase with depth in soils (Krüger et al., 2023;
412 Natelhoffer & Fry, 1988; Staddon, 2004); however, Hopland had lower $\delta^{13}C$ values in depths greater than 30cm, but
413 Angelo and Sedgwick had relatively similar values. Our range of $\delta^{13}C$ values were relatively similar to other C3
414 dominant grassland sites (Brenner et al., 2001; Schneckenberger & Kuzyakov, 2007; Von Fischer et al., 2008; Wedin
415 et al., 1995). At Hopland, the intermediate temperature and precipitation site, we observed the lowest $\delta^{13}C$ values
416 below 30cm (fig. 3d) and redoximorphic features at depth (~60-100cm). There is emerging evidence that microbial
417 necromass contributes to $\delta^{13}C$ values, especially at depth (Kohl et al., 2015). High $\delta^{13}C$ values are indicative of a
418 greater isotopic fractionation that occurs during microbial carbon recycling and necromass accumulation (Krüger et
419 al., 2023). The redox features at Hopland are evidence of a mixture of oxic and anoxic microsites within soil. These
420 microsites have been shown to have a higher diversity of aerobic and anaerobic microbial metabolisms and metabolites
421 are key in soil carbon stabilization (Keiluweit et al., 2017; Lacroix et al., 2023; Naughton et al., 2023), but the
422 connection between $\delta^{13}C$ values and reactive microsites is not well characterized. This chemical process could explain
423 the divergence of Hopland in its $\delta^{13}C$ values in soil depths greater than 30cm (fig. 3d) and the broadest variability in
424 complex plant derived OM at depth (fig. 6c).
425 In contrast to our initial hypothesis, we did not observe a strong relationship between $\delta^{15}N$ values across our
426 grassland ecosystems with varying precipitation regimes. This lack of $\delta^{15}N$ variation with climate is consistent with
427 previous findings that suggest that $\delta^{15}N$ is invariant with MAP after controlling for soil carbon and clay content (Craine
428 et al., 2015). These samples were collected during the peak of dry season in Mediterranean grasslands when we would
429 expect lower microbial activity compared to the wet winter season. Studies have found that soil $\delta^{15}N$ values at depth
430 in regions with a distinct wet and dry season are greatly affected by time of sampling (Wang et al., 2009). It is common
431 for grasslands to exhibit a consistent increase of $\delta^{15}N$ values with depth (Amundson et al., 2003) but during the wet
432 season, , $\delta^{15}N$ values decrease at the surface due to higher levels of microbial activity and $^{14}N$ loss, which results in
433 $^{15}N$ enriched substrates (L. Wang et al., 2009). Another biotic process that can affect $\delta^{15}N$ depth profiles is fungal
434 inputs. Soil $\delta^{15}N$ values at depth integrate many processes and can be dominated by fungal transfer of nitrogen to
435 plants; however, typical soil processing protocols bias against observing root inputs in samples due to sieving (Hobbie

& Ouimette, 2009). Ecosystems with arbuscular mycorrhizal (AMF) fungi have $\delta^{15}N$ values of 4.6±0.5‰ and maximum values at intermediate depth (Hobbie & Ouimette, 2009). At Hopland, we observed this $\delta^{15}N$ profile pattern consistent with AMF processes. The prevalence of AMF at all three of our study sites is well documented through amplicon sequencing (Hawkes et al., 2011; Treseder et al., 2010; Yuan et al., 2021) but determining the effects of AMF on $\delta^{15}N$ profiles will take further investigation. Lastly, $\delta^{15}N$ values can be affected by abiotic inputs, namely rock derived nitrogen, as documented at Sedgwick where there are high $\delta^{15}N$ values (~6‰) at depths greater than 1m (Bingham et al., 2021). While our results did not directly indicate rock derived nitrogen at Sedgwick, there were increased $\delta^{15}N$ values at depth and we cannot rule out this impact.

### 4.3 Climatic factors may explain differences in processing index across ecosystems, but not in turnover index

Angelo, Hopland, and Sedgwick represent a climatic gradient of grassland ecosystems and we observed unique patterns in stabilization mechanisms and microbial processing through their depth profiles of C:N and stable isotopes. Stability, or persistence, of soil organic matter has emerged as an important ecosystem property in the current paradigm of soil science research (Schmidt et al., 2011). Relationships between C:N and $\delta^{15}N$ values coincides with measurements of mineral-associated versus particulate organic matter (POM) (Conen et al., 2008). At Angelo, subsoil (>30cm) SOM was largely differentiated by depth separation of C:N, indicating carbon loss at depth with not much variation in $\delta^{15}N$ (fig. 6a). More specifically, the differentiation in patterns of C:N and $\delta^{15}N$ values between shallow versus deep soils at Angelo suggests the dominant mechanism of stabilization is through mineral association with iron and aluminum short-range order oxides (Berhe et al., 2012; Foley et al., 2023). In contrast, at Sedgwick, there was a homogenous, continuous $\delta^{15}N$ and C:N association across all depths, with a high variability in $\delta^{15}N$ values and little depth separation (Conen et al., 2008). We interpret this as indicative of greater microbial processing at Sedgwick and differing stabilization mechanisms at our sites. Sedgwick has a higher pH and higher clay content at the surface (table 1), and stabilization here is likely driven by organic matter association with polyvalent base cations. Our results also agree with prior studies and strengthen the hypothesis that wetter environments lead to stabilization of organic matter and more MAOM formation (Heckman et al., 2023).

Differences in soil turnover across the study sites, interpreted through the turnover index ($\beta$), were decoupled from climatic differences across sites. We observed highest turnover at Sedgwick, our driest site (fig. 5a). Previous studies indicate an inverse relationship between MAT and $\beta$ (Brunn et al., 2014); however, Sedgwick and Angelo

had similar $\beta$ values, which is inconsistent with previous studies corresponding increases in $\beta$ with MAP (Brunn et al., 2014). The majority of previous studies regarding $\beta$ have been done in temperate forest ecosystems (fig. S3), which likely affects the relationship between $\beta$ and climate. However, our data fall within expected values for other temperate ecosystems (fig. S3). Additionally, greater decomposition rate under higher MAP is not consistent in the literature, however our relative turnover times also agree with Foley et al. (2023) that reported radiocarbon ($^{14}C$) age of surface soils at these same three localities and observed increases in $^{14}C$ age with MAP. These younger soil C ages at Sedgwick provide evidence for greater microbial processing of organic matter at Sedgwick (Foley et al., 2023). $\delta^{13}C$ values are connected to decomposition processes in soils, and can be affected by the interactions between litter quality, microbial respiration, and the physiochemical parameters of soil (Brunn et al., 2014). The increase in $\beta$ at Angelo could also be due to leaching of dissolved organic carbon (DOC), which is possible due to its precipitation regime and high relative MAP (fig. 1a). Increased DOC leaching through the profile can increase $\beta$ due to the $^{13}C$ enrichment (Kaiser & Zech, 2000); however, recent studies have questioned this $^{13}C$ enrichment of DOC (Philben et al., 2022). Instead, $^{13}C$ enrichment is likely dominated by biotic factors, like microbial immobilization, plant uptake, and fungal transport (Philben et al., 2022). High $\beta$ at Sedgwick is also consistent with our DRIFTS data in Sedgwick subsoils, which suggests greater microbial oxidation in subsoils (fig. 5) compared to Angelo.

This study combines the geochemical and spectrographic techniques of stable isotope analysis and DRIFTS to determine proxies of processing and turnover of soil carbon, as well as to discern the contributing biological processes. A standard and accepted method for determining stability is splitting SOC into mineral-associated and particulate organic carbon, via a costly and labor-intensive density fractionation methodology (Sollins et al., 2006, 2009). Turnover is commonly assessed through radiocarbon measurements, which is inaccessible to many researchers given the cost and limited availability of specialized instrumentation. Analysis of elemental concentrations and stable isotope compositions using elemental analyzers coupled to isotope ratio mass spectrometers are increasingly becoming more common and affordable. In contrast to density fractionation and radiocarbon measurement, stable isotope proxies can be used as a high throughput and low-cost way to measure benchmarks for important ecosystem properties like soil turnover and stability. The non-destructive acquisition of DRIFTS data was suitable for detecting regional differences in functional group character between sites and at picking up depth differences (fig. 7,8). Combining isotopic proxies and spectroscopic methods can be another powerful and accessible way of understanding carbon and nitrogen dynamics across diverse ecosystems.

### 4.4 Implications for grassland C sequestration

The effect of changing precipitation and temperature patterns on terrestrial carbon cycling will have cascading consequences for soil carbon sequestration (Bai & Cotrufo, 2022; Song et al., 2019). Plant communities are affected by both the amount and timing of precipitation. In tall-grass prairie ecosystems, decreases in precipitation result in lower plant diversity (Dennhardt et al., 2021; Fay et al., 2002; Smith et al., 2016). Shifts in diversity as well as increases in invasives annuals in California grasslands are associated with declines in soil C storage (Koteen et al., 2011). There is also evidence from Angelo that extending the rainy season into the spring has increased the dominance of invasive annual grasses (Suttle et al., 2007). Overall, this linkage between reduced plant diversity and SOC storage in California grasslands suggests a negative impact on their capacity to sequester atmospheric carbon dioxide. In this study, we illustrated regional differences in SOM processing, turnover, and composition. Although we did not observe large differences in elemental concentration of carbon and nitrogen, we detected differences in the processing of carbon at depth across the sites. These regional differences in baseline processing, turnover, and organic matter composition need to be taken into account for future C sequestration and modeling efforts.

## 5 Conclusions

We investigated the SOM processing, turnover, and organic matter composition down to 1 m depths across three Californian grassland ecosystems. Elemental and isotopic analysis reveal that, while there are few differences in carbon and nitrogen abundances in grassland soils, we do see differences in the processing and turnover of SOM across a mean annual precipitation gradient. We applied two natural isotopic abundance proxies as an index for turnover ($\boldsymbol{\beta}$) and processing (C:N versus $\delta^{15}N$). We also characterized organic matter composition using Diffuse Reflectance Infrared Fourier Transform Spectroscopy (DRIFTS) to better characterize the plant and microbial character across gradients and depths. Our results found the wettest site had the greatest carbon stock at the surface, likely mediated by greater plant inputs; however, carbon stock values converged between the wettest and driest site in subsoils. Soil at the driest and hottest site (Sedgwick) has the greatest turnover and most processing. The wettest site (Angelo) had a high degree of processing at depth, likely due to greater mineral association of organic matter at depth. We observed the lowest $\delta^{13}C$ values in subsoils at our intermediate site, despite expecting the greatest values at our driest site. Our results highlight regional variability in SOM processing and turnover across climatic gradients. The

contrasting results between topsoils and subsoils demonstrate the importance of understanding both regional differences and patterns with depth across a climatic gradient of California grasslands.

## Acknowledgments

We thank Debbo Elias, Charlotte Calvario, Todd Longbottom, Ronnie Hall, Xin Gao, and Jing Yan for assistance in field sampling and lab analyses. In addition, this study would not be possible without the field support from John Bailey at Hopland Research and Extension Center, Peter Steel from Angelo Coast Range Reserve, and Kate McCurdy at Sedgwick reserve, especially in August 2020 during the COVID-19 pandemic. This research was supported by the Department of Energy, Sigma Xi Grants in Aid of Research, the UC Natural Reserve System Mathias Grant, and a UC Merced Committee on Research Senate Award. We thank Dr. Jennifer Pett-Ridge for help in experimental design and setup. We would also like to thank Dr. Teamrat Ghezzehei for his invaluable guidance. This research was supported by the U.S. Department of Energy, Office of Biological and Environmental Research, Genomic Science Program 'Microbes Persist' Scientific Focus Area (#SCW1632) at Lawrence Livermore National Laboratory (LLNL).

**References**

Abdelbaki, A. M. (2018). Evaluation of pedotransfer functions for predicting soil bulk density for U.S. soils. *Ain Shams Engineering Journal*, *9*(4), 1611–1619. https://doi.org/10.1016/j.asej.2016.12.002

Acton, P., Fox, Campbell, E., Rowe, H., & Wilkinson, M. (2013). Carbon isotopes for estimating soil decomposition and physical mixing in well-drained forest soils. *JGR: Biogeosciences*, *118*, 1532–1545. https://doi.org/doi:10.1002/2013JG002400

Agnihotri, R., Mandal, T. K., Karapurkar, S. G., Naja, M., Gadi, R., Ahammmed, Y. N., Kumar, A., Saud, T., & Saxena, M. (2011). Stable carbon and nitrogen isotopic composition of bulk aerosols over India and northern Indian Ocean. *Atmospheric Environment*, *45*(17), 2828–2835. https://doi.org/10.1016/j.atmosenv.2011.03.003

Alexander, E. B. (1980). Bulk Densities of California Soils in Relation to Other Soil Properties. *Soil Science Society of America Journal*, *44*(4), 689–692. https://doi.org/10.2136/sssaj1980.03615995004400040005x

Amundson, R., Austin, A. T., Schuur, E. A. G., Yoo, K., Matzek, V., Kendall, C., Uebersax, A., Brenner, D., & Baisden, W. T. (2003). Global patterns of the isotopic composition of soil and plant nitrogen. *Global Biogeochemical Cycles*, *17*(1). https://doi.org/10.1029/2002GB001903

Aquino, A. J. A., Tunega, D., Schaumann, G. E., Haberhauer, G., Gerzabek, M. H., & Lischka, H. (2011). The functionality of cation bridges for binding polar groups in soil aggregates. *International Journal of Quantum Chemistry*, *111*(7–8), 1531–1542. https://doi.org/10.1002/qua.22693

Aranibar, J. N., Otter, L., Macko, S. A., Feral, C. J. W., Epstein, H. E., Dowty, P. R., Eckardt, F., Shugart, H. H., & Swap, R. J. (2004). Nitrogen cycling in the soil-plant system along a precipitation gradient in the Kalahari sands: NITROGEN CYCLING IN THE KALAHARI. *Global Change Biology*, *10*(3), 359–373. https://doi.org/10.1111/j.1365-2486.2003.00698.x

Bai, Y., & Cotrufo, M. F. (2022). Grassland soil carbon sequestration: Current understanding, challenges, and solutions. *Science*, *377*(6606), 603–608. https://doi.org/10.1126/science.abo2380

Berhe, A., Suttle, K. B., Burton, S. D., & Banfield, J. F. (2012). Contingency in the direction and mechanics of soil organic matter responses to increased rainfall. *Plant and Soil*, *358*.

Berthrong, S. T., Piñeiro, G., Jobbágy, E. G., & Jackson, R. B. (2012). Soil C and N changes with afforestation of grasslands across gradients of precipitation and plantation age. *Ecological Applications*, *22*(1), 76–86. https://doi.org/10.1890/10-2210.1

Bingham, N. L., Slessarev, E. W., Homyak, P. M., & Chadwick, O. A. (2021). Rock-Sourced Nitrogen in Semi-Arid, Shale-Derived California Soils. *Frontiers in Forests and Global Change*, *4*, 672522. https://doi.org/10.3389/ffgc.2021.672522

564 Brenner, D. L., Amundson, R., Baisden, W. T., Kendall, C., & Harden, J. (2001). Soil N and 15 N variation with
565 time in a California annual grassland ecosystem. *Geochimica et Cosmochimica Acta*, *65*(22), 4171–4186.
566 https://doi.org/10.1016/S0016-7037(01)00699-8
567 Brunn, M., Condron, L., Wells, A., Spielvogel, S., & Oelmann, Y. (2016). Vertical distribution of carbon and
568 nitrogen stable isotope ratios in topsoils across a temperate rainforest dune chronosequence in New
569 Zealand. *Biogeochemistry*, *129*(1–2), 37–51. https://doi.org/10.1007/s10533-016-0218-4
570 Brunn, M., Spielvogel, S., Sauer, T., & Oelmann, Y. (2014). Temperature and precipitation effects on δ13C depth
571 profiles in SOM under temperate beech forests. *Geoderma*, *235–236*, 146–153.
572 https://doi.org/10.1016/j.geoderma.2014.07.007
573 Buckeridge, K. M., La Rosa, A. F., Mason, K. E., Whitaker, J., McNamara, N. P., Grant, H. K., & Ostle, N. J.
574 (2020). Sticky dead microbes: Rapid abiotic retention of microbial necromass in soil. *Soil Biology and*
575 *Biochemistry*, *149*, 107929. https://doi.org/10.1016/j.soilbio.2020.107929
576 Buckeridge, K. M., Mason, K. E., Ostle, N., McNamara, N. P., Grant, H. K., & Whitaker, J. (2022). Microbial
577 necromass carbon and nitrogen persistence are decoupled in agricultural grassland soils. *Communications*
578 *Earth & Environment*, *3*(1), 114. https://doi.org/10.1038/s43247-022-00439-0
579 Button, E. S., Pett-Ridge, J., Murphy, D. V., Kuzyakov, Y., Chadwick, D. R., & Jones, D. L. (2022). Deep-C
580 storage: Biological, chemical and physical strategies to enhance carbon stocks in agricultural subsoils. *Soil*
581 *Biology and Biochemistry*, *170*, 108697. https://doi.org/10.1016/j.soilbio.2022.108697
582 Campbell, J. E., Fox, J. F., Davis, C. M., Rowe, H. D., & Thompson, N. (2009). Carbon and Nitrogen Isotopic
583 Measurements from Southern Appalachian Soils: Assessing Soil Carbon Sequestration under Climate and
584 Land-Use Variation. *Journal of Environmental Engineering*, *135*(6), 439–448.
585 https://doi.org/10.1061/(ASCE)EE.1943-7870.0000008
586 Campo, J., & Merino, A. (2016). Variations in soil carbon sequestration and their determinants along a precipitation
587 gradient in seasonally dry tropical forest ecosystems. *Global Change Biology*, *22*(5), 1942–1956.
588 https://doi.org/10.1111/gcb.13244
589 Chai, H., Li, J., Ochoa-Hueso, R., Yang, X., Li, J., Meng, B., Song, W., Zhong, X., Ma, J., & Sun, W. (2022).
590 Different drivers of soil C accumulation in aggregates in response to altered precipitation in a semiarid
591 grassland. *Science of The Total Environment*, *830*, 154760. https://doi.org/10.1016/j.scitotenv.2022.154760
592 Chen, J., Elsgaard, L., Van Groenigen, K. J., Olesen, J. E., Liang, Z., Jiang, Y., Lærke, P. E., Zhang, Y., Luo, Y.,
593 Hungate, B. A., Sinsabaugh, R. L., & Jørgensen, U. (2020). Soil carbon loss with warming: New evidence
594 from carbon-degrading enzymes. *Global Change Biology*, *26*(4), 1944–1952.
595 https://doi.org/10.1111/gcb.14986
596 Chen, J., van Groenigen, K. J., Hungate, B. A., Terrer, C., van Groenigen, J.-W., Maestre, F. T., Ying, S. C., Luo,
597 Y., Jørgensen, U., & Sinsabaugh, R. L. (2020). Long-term nitrogen loading alleviates phosphorus limitation
598 in terrestrial ecosystems. *Global Change Biology*, *26*(9), 5077–5086.
599 Chou, W. W., Silver, W. L., Jackson, R. D., Thompson, A. W., & Allen-Diaz, B. (2008). The sensitivity of annual
600 grassland carbon cycling to the quantity and timing of rainfall. *Global Change Biology*, *14*(6), 1382–1394.
601 https://doi.org/10.1111/j.1365-2486.2008.01572.x
602 Conen, F., Yakutin, M. V., Carle, N., & Alewell, C. (2013). δ $^{15}$ N natural abundance may directly disclose
603 perturbed soil when related to C:N ratio: δ $^{15}$ N natural abundance to directly disclose perturbed soil. *Rapid*
604 *Communications in Mass Spectrometry*, *27*(10), 1101–1104. https://doi.org/10.1002/rcm.6552
605 Conen, F., Zimmermann, M., Leifeld, J., Seth, B., & Alewell, C. (2008). *Relative stability of soil carbon revealed by*
606 *shifts in δ15N and C:N ratio*. 6.
607 Craine, J. M., Elmore, A. J., Wang, L., Augusto, L., Baisden, W. T., Brookshire, E. N. J., Cramer, M. D.,
608 Hasselquist, N. J., Hobbie, E. A., Kahmen, A., Koba, K., Kranabetter, J. M., Mack, M. C., Marin-Spiotta,
609 E., Mayor, J. R., McLauchlan, K. K., Michelsen, A., Nardoto, G. B., Oliveira, R. S., … Zeller, B. (2015).
610 Convergence of soil nitrogen isotopes across global climate gradients. *Scientific Reports*, *5*(1), 8280.
611 https://doi.org/10.1038/srep08280
612 D'Antonio, C., Bainbridge, S., Kennedy, C., Bartolome, J., & Reynolds, S. (2002). Ecology and Restoration of
613 California Grasslands with special emphasis on the influence of fire and grazing on native grassland
614 species. *Report to the Packard Foundation*, 99.
615 Deepika, S., & Kothamasi, D. (2015). Soil moisture—A regulator of arbuscular mycorrhizal fungal community
616 assembly and symbiotic phosphorus uptake. *Mycorrhiza*, *25*(1), 67–75. https://doi.org/10.1007/s00572-
617 014-0596-1

Dennhardt, L. A., Aldrich-Wolfe, L., Black, K. L., Shivega, W. G., & Travers, S. E. (2021). Forty Years of Increasing Precipitation is Correlated with Loss of Forbs in a Tallgrass Prairie. *Natural Areas Journal*, *41*(3). https://doi.org/10.3375/043.041.0305

Ehleringer, J. R., Buchmann, N., & Flanagan, L. B. (2000). CARBON ISOTOPE RATIOS IN BELOWGROUND CARBON CYCLE PROCESSES. *Ecological Applications*, *10*(2), 412–422. https://doi.org/10.1890/1051-0761(2000)010[0412:CIRIBC]2.0.CO;2

Farquhar, G. D., Ehleringer, J. R., & Hubick, K. T. (1989). Carbon Isotope Discrimination and Photosynthesis. *Annual Review Plant Physiology and Plant Molecular Biology*, *40*, 503–537.

Fay, P. A., Carlisle, J. D., Danner, B. T., Lett, M. S., McCarron, J. K., Stewart, C., Knapp, A. K., Blair, J. M., & Collins, S. L. (2002). Altered Rainfall Patterns, Gas Exchange, and Growth in Grasses and Forbs. *International Journal of Plant Sciences*, *163*(4), 549–557. https://doi.org/10.1086/339718

Foley, M. M., Blazewicz, S. J., McFarlane, K. J., Greenlon, A., Hayer, M., Kimbrel, J. A., Koch, B. J., Monsaint-Queeney, V. L., Morrison, K., Morrissey, E., Hungate, B. A., & Pett-Ridge, J. (2023). Active populations and growth of soil microorganisms are framed by mean annual precipitation in three California annual grasslands. *Soil Biology and Biochemistry*, *177*, 108886. https://doi.org/10.1016/j.soilbio.2022.108886

Fröberg, M., Hanson, P. J., Todd, D. E., & Johnson, D. W. (2008). Evaluation of effects of sustained decadal precipitation manipulations on soil carbon stocks. *Biogeochemistry*, *89*(2), 151–161. https://doi.org/10.1007/s10533-008-9205-8

Garten, C. T. (2006). *Relationships among forest soil C isotopic composition, partitioning, and turnover times*. *36*, 11.

Garten, C. T., & Hanson, P. J. (2006). Measured forest soil C stocks and estimated turnover times along an elevation gradient. *Geoderma*, *136*(1–2), 342–352. https://doi.org/10.1016/j.geoderma.2006.03.049

Grant, K. E., Hilton, R. G., & Galy, V. V. (2023). Global patterns of radiocarbon depletion in subsoil linked to rock-derived organic carbon. *Geochemical Perspectives Letters*, *25*, 36–40. https://doi.org/10.7185/geochemlet.2312

Harper, C. W., Blair, J. M., Fay, P. A., Knapp, A. K., & Carlisle, J. D. (2005). Increased rainfall variability and reduced rainfall amount decreases soil CO2 flux in a grassland ecosystem. *Global Change Biology*, *11*(2), 322–334. https://doi.org/10.1111/j.1365-2486.2005.00899.x

Hartman, G., & Danin, A. (2010). Isotopic values of plants in relation to water availability in the Eastern Mediterranean region. *Oecologia*, *162*(4), 837–852. https://doi.org/10.1007/s00442-009-1514-7

Hawkes, C. V., Kivlin, S. N., Rocca, J. D., Huguet, V., Thomsen, M. A., & Suttle, K. B. (2011). Fungal Community Responses to Precipitation. *Global Change Biology*, *17*(4), 1637–1645. https://doi.org/10.1111/j.1365-2486.2010.02327.x

Heckman, K. A., Possinger, A. R., Badgley, B. D., Bowman, M. M., Gallo, A. C., Hatten, J. A., Nave, L. E., SanClements, M. D., Swanston, C. W., Weiglein, T. L., Wieder, W. R., & Strahm, B. D. (2023). Moisture-driven divergence in mineral-associated soil carbon persistence. *Proceedings of the National Academy of Sciences*, *120*(7), e2210044120. https://doi.org/10.1073/pnas.2210044120

Hicks Pries, C. E., Ryals, R., Zhu, B., Min, K., Cooper, A., Goldsmith, S., Pett-Ridge, J., Torn, M., & Berhe, A. A. (2023). The Deep Soil Organic Carbon Response to Global Change. *Annual Review of Ecology, Evolution, and Systematics*, *54*(1), 375–401. https://doi.org/10.1146/annurev-ecolsys-102320-085332

Hobbie, E. A., & Ouimette, A. P. (2009a). Controls of nitrogen isotope patterns in soil profiles. *Biogeochemistry*, *95*(2–3), 355–371. https://doi.org/10.1007/s10533-009-9328-6

Hobbie, E. A., & Ouimette, A. P. (2009b). Controls of nitrogen isotope patterns in soil profiles. *Biogeochemistry*, *95*(2–3), 355–371. https://doi.org/10.1007/s10533-009-9328-6

Högberg, P. (1997). 15N natural abundance in soil–plant systems. *The New Phytologist*, *137*(2), 179–203.

IPCC. (2014). *Climate Change 2014: Impacts, Adaptation, and Vulnerability. Part A: Global and Sectoral Aspects. Contribution of Working Group II to the Fifth Assessment Report of the Intergovernmental Panel on Climate Change*.

IPCC. (2022). *Water. In: Climate Change 2022: Impacts, Adaptation, and Vulnerability. Contribution of Working Group II to the Sixth Assessment Report of the Intergovernmental Panel on Climate Change*.

Jia, J., Cao, Z., Liu, C., Zhang, Z., Lin, L., Wang, Y., Haghipour, N., Wacker, L., Bao, H., Dittmar, T., Simpson, M. J., Yang, H., Crowther, T. W., Eglinton, T. I., He, J., & Feng, X. (2019). Climate warming alters subsoil but not topsoil carbon dynamics in alpine grassland. *Global Change Biology*, *25*(12), 4383–4393. https://doi.org/10.1111/gcb.14823

Jilling, A., Keiluweit, M., Contosta, A. R., Frey, S., Schimel, J., Schnecker, J., Smith, R. G., Tiemann, L., & Grandy, A. S. (2018). Minerals in the rhizosphere: Overlooked mediators of soil nitrogen availability to plants and microbes. *Biogeochemistry*, *139*(2), 103–122. https://doi.org/10.1007/s10533-018-0459-5

Jobbágy, E. G., & Jackson, R. B. (2000). THE VERTICAL DISTRIBUTION OF SOIL ORGANIC CARBON AND ITS RELATION TO CLIMATE AND VEGETATION. *Ecological Applications*, *10*(2), 423–436. https://doi.org/10.1890/1051-0761(2000)010[0423:TVDOSO]2.0.CO;2

Kaiser, K., & Zech, W. (2000). Sorption of dissolved organic nitrogen by acid subsoil horizons and individual mineral phases. *European Journal of Soil Science*, *51*(3), 403–411. https://doi.org/10.1046/j.1365-2389.2000.00320.x

Keiluweit, M., Wanzek, T., Kleber, M., Nico, P., & Fendorf, S. (2017). Anaerobic microsites have an unaccounted role in soil carbon stabilization. *Nature Communications*, *8*(1), 1771. https://doi.org/10.1038/s41467-017-01406-6

Knapp, A. K. (2002). Rainfall Variability, Carbon Cycling, and Plant Species Diversity in a Mesic Grassland. *Science*, *298*(5601), 2202–2205. https://doi.org/10.1126/science.1076347

Kohl, L., Laganière, J., Edwards, K. A., Billings, S. A., Morrill, P. L., Van Biesen, G., & Ziegler, S. E. (2015). Distinct fungal and bacterial δ13C signatures as potential drivers of increasing δ13C of soil organic matter with depth. *Biogeochemistry*, *124*(1–3), 13–26. https://doi.org/10.1007/s10533-015-0107-2

Kohn, M. J. (2010). Carbon isotope compositions of terrestrial C3 plants as indicators of (paleo)ecology and (paleo)climate. *Proceedings of the National Academy of Sciences*, *107*(46), 19691–19695. https://doi.org/10.1073/pnas.1004933107

Koteen, L. E., Baldocchi, D. D., & Harte, J. (2011). Invasion of non-native grasses causes a drop in soil carbon storage in California grasslands. *Environmental Research Letters*, *6*(4), 044001. https://doi.org/10.1088/1748-9326/6/4/044001

Krüger, N., Finn, D. R., & Don, A. (2023). Soil depth gradients of organic carbon-13 – A review on drivers and processes. *Plant and Soil*. https://doi.org/10.1007/s11104-023-06328-5

Lacroix, E. M., Aeppli, M., Boye, K., Brodie, E., Fendorf, S., Keiluweit, M., Naughton, H. R., Noël, V., & Sihi, D. (2023). Consider the Anoxic Microsite: Acknowledging and Appreciating Spatiotemporal Redox Heterogeneity in Soils and Sediments. *ACS Earth and Space Chemistry*, *7*(9), 1592–1609. https://doi.org/10.1021/acsearthspacechem.3c00032

Liang, C., Amelung, W., Lehmann, J., & Kästner, M. (2019). Quantitative assessment of microbial necromass contribution to soil organic matter. *Global Change Biology*, *25*(11), 3578–3590. https://doi.org/10.1111/gcb.14781

Mainka, M., Summerauer, L., Wasner, D., Garland, G., Griepentrog, M., Berhe, A. A., & Doetterl, S. (2021). *Soil geochemistry as a driver of soil organic matter composition: Insights from a soil chronosequence* [Preprint]. Biogeochemistry: Soils. https://doi.org/10.5194/bg-2021-295

Margenot, A., Calderón, F., & Parikh, S. J. (2015). Limitations and Potential of Spectral Subtractions in Fourier-Transform Infrared Spectroscopy of Soil Samples. *Soil Science Society of America Journal*, *80*, 10–26. https://doi.org/10.2136/sssaj2015.06.0228

Natelhoffer, K. J., & Fry, B. (1988). Controls on Natural Nitrogen-15 and Carbon-13 Abundances in Forest Soil Organic Matter. *Soil Science Society of America Journal*, *52*(6).

Naughton, H. R., Tolar, B. B., Dewey, C., Keiluweit, M., Nico, P. S., & Fendorf, S. (2023). Reactive iron, not fungal community, drives organic carbon oxidation potential in floodplain soils. *Soil Biology and Biochemistry*, *178*, 108962. https://doi.org/10.1016/j.soilbio.2023.108962

Parikh, S. J., Goyne, K. W., Margenot, A. J., Mukome, F. N. D., & Calderón, F. J. (2014). Soil Chemical Insights Provided through Vibrational Spectroscopy. In *Advances in Agronomy* (Vol. 126, pp. 1–148). Elsevier. https://doi.org/10.1016/B978-0-12-800132-5.00001-8

Philben, M., Bowering, K., Podrebarac, F. A., Laganière, J., Edwards, K., & Ziegler, S. E. (2022). Enrichment of 13C with depth in soil organic horizons is not explained by CO2 or DOC losses during decomposition. *Geoderma*, *424*, 116004. https://doi.org/10.1016/j.geoderma.2022.116004

Robinson, D. (2001). δ15N as an integrator of the nitrogen cycle. *Trends in Ecology & Evolution*, *16*(3), 153–162. https://doi.org/10.1016/S0169-5347(00)02098-X

Rocci, K. S., Lavallee, J. M., Stewart, C. E., & Cotrufo, M. F. (2021). Soil organic carbon response to global environmental change depends on its distribution between mineral-associated and particulate organic matter: A meta-analysis. *Science of The Total Environment*, *793*, 148569. https://doi.org/10.1016/j.scitotenv.2021.148569

Rumpel, C. (2004). Location and chemical composition of stabilized organic carbon in topsoil and subsoil horizons of two acid forest soils. *Soil Biology and Biochemistry*, *36*(1), 177–190. https://doi.org/10.1016/j.soilbio.2003.09.005

Schmidt, M. W. I., Torn, M. S., Abiven, S., Dittmar, T., Guggenberger, G., Janssens, I. A., Kleber, M., Kögel-Knabner, I., Lehmann, J., Manning, D. A. C., Nannipieri, P., Rasse, D. P., Weiner, S., & Trumbore, S. E. (2011). Persistence of soil organic matter as an ecosystem property. *Nature*, *478*(7367), 49–56. https://doi.org/10.1038/nature10386

Schneckenberger, K., & Kuzyakov, Y. (2007). Carbon sequestration under *Miscanthus* in sandy and loamy soils estimated by natural $^{13}$C abundance. *Journal of Plant Nutrition and Soil Science*, *170*(4), 538–542. https://doi.org/10.1002/jpln.200625111

Smith, N. G., Schuster, M. J., & Dukes, J. S. (2016). Rainfall variability and nitrogen addition synergistically reduce plant diversity in a restored tallgrass prairie. *Journal of Applied Ecology*, *53*(2), 579–586. https://doi.org/10.1111/1365-2664.12593

Sokol, N. W., Whalen, E., Jilling, A., Kallenbach, C. M., Pett-Ridge, J., & Georgiou, K. (2022). Global distribution, formation and fate of mineral-associated soil organic matter under a changing climate: A trait-based perspective. *Functional Ecology*, *36*, 1411–1429. https://doi.org/10.1111/1365-2435.14040

Sollins, P., Kramer, M. G., Swanston, C., Lajtha, K., Filley, T., Aufdenkampe, A. K., Wagai, R., & Bowden, R. D. (2009). Sequential density fractionation across soils of contrasting mineralogy: Evidence for both microbial- and mineral-controlled soil organic matter stabilization. *Biogeochemistry*, *96*(1–3), 209–231. https://doi.org/10.1007/s10533-009-9359-z

Sollins, P., Swanston, C., Kleber, M., Filley, T., Kramer, M., Crow, S., Caldwell, B. A., Lajtha, K., & Bowden, R. (2006). Organic C and N stabilization in a forest soil: Evidence from sequential density fractionation. *Soil Biology and Biochemistry*, *38*(11), 3313–3324. https://doi.org/10.1016/j.soilbio.2006.04.014

Song, J., Wan, S., Piao, S., Knapp, A. K., Classen, A. T., Vicca, S., Ciais, P., Hovenden, M. J., Leuzinger, S., Beier, C., Kardol, P., Xia, J., Liu, Q., Ru, J., Zhou, Z., Luo, Y., Guo, D., Adam Langley, J., Zscheischler, J., … Zheng, M. (2019). A meta-analysis of 1,119 manipulative experiments on terrestrial carbon-cycling responses to global change. *Nature Ecology & Evolution*, *3*(9), 1309–1320. https://doi.org/10.1038/s41559-019-0958-3

Staddon, P. L. (2004). Carbon isotopes in functional soil ecology. *Trends in Ecology & Evolution*, *19*(3), 148–154. https://doi.org/10.1016/j.tree.2003.12.003

Suttle, K. B., & Thomsen, M. A. (2007). Climate Change and Grassland Restoiration in California: Lessons from Six Years of Rainfall Manipulation in a North Coast Grassland. *Madroño*, *54*(3), 225–233. https://doi.org/10.3120/0024-9637(2007)54[225:CCAGRI]2.0.CO;2

Suttle, K. B., Thomsen, M. A., & Power, M. E. (2007). Species Interactions Reverse Grassland Responses to Changing Climate. *Science*, *315*(5812), 640–642. https://doi.org/10.1126/science.1136401

Terrer, C., Phillips, R. P., Hungate, B. A., Rosende, J., Pett-Ridge, J., Craig, M. E., van Groenigen, K. J., Keenan, T. F., Sulman, B. N., Stocker, B. D., Reich, P. B., Pellegrini, A. F. A., Pendall, E., Zhang, H., Evans, R. D., Carrillo, Y., Fisher, J. B., Van Sundert, K., Vicca, S., & Jackson, R. B. (2021). A trade-off between plant and soil carbon storage under elevated CO2. *Nature*, *591*(7851), 599–603. https://doi.org/10.1038/s41586-021-03306-8

Throop, H. L., Archer, S. R., Monger, H. C., & Waltman, S. (2012). When bulk density methods matter: Implications for estimating soil organic carbon pools in rocky soils. *Journal of Arid Environments*, *77*, 66–71. https://doi.org/10.1016/j.jaridenv.2011.08.020

Treseder, K. K., Schimel, J. P., Garcia, M. O., & Whiteside, M. D. (2010). Slow turnover and production of fungal hyphae during a Californian dry season. *Soil Biology and Biochemistry*, *42*(9), 1657–1660. https://doi.org/10.1016/j.soilbio.2010.06.005

Von Fischer, J. C., Tieszen, L. L., & Schimel, D. S. (2008). Climate controls on $C_3$ vs. $C_4$ productivity in North American grasslands from carbon isotope composition of soil organic matter. *Global Change Biology*, *14*(5), 1141–1155. https://doi.org/10.1111/j.1365-2486.2008.01552.x

Vranova, V., Rejsek, K., & Formanek, P. (2013). Aliphatic, Cyclic, and Aromatic Organic Acids, Vitamins, and Carbohydrates in Soil: A Review. *The Scientific World Journal*, *2013*, 1–15. https://doi.org/10.1155/2013/524239

Wang, B., An, S., Liang, C., Liu, Y., & Kuzyakov, Y. (2021). Microbial necromass as the source of soil organic carbon in global ecosystems. *Soil Biology and Biochemistry*, *162*, 108422. https://doi.org/10.1016/j.soilbio.2021.108422

Wang, C., Houlton, B. Z., Liu, D., Hou, J., Cheng, W., & Bai, E. (2018). Stable isotopic constraints on global soil organic carbon turnover. *Biogeosciences*, *15*(4), 987–995. https://doi.org/10.5194/bg-15-987-2018

Wang, L., D'Odorico, P., Okin, G. S., & Macko, S. A. (2009). Isotope composition and anion chemistry of soil profiles along the Kalahari Transect. *Journal of Arid Environments*, *73*(4–5), 480–486. https://doi.org/10.1016/j.jaridenv.2008.11.010

Wedin, D. A., Tieszen, L. L., Dewey, B., & Pastor, J. (1995). Carbon Isotope Dynamics During Grass Decomposition and Soil Organic Matter Formation. *Ecology*, *76*(5), 1383–1392. https://doi.org/10.2307/1938142

Yost, J. L., & Hartemink, A. E. (2020). How deep is the soil studied – an analysis of four soil science journals. *Plant and Soil*, *452*(1–2), 5–18. https://doi.org/10.1007/s11104-020-04550-z

Yuan, M. M., Kakouridis, A., Starr, E., Nguyen, N., Shi, S., Pett-Ridge, J., Nuccio, E., Zhou, J., & Firestone, M. (2021). Fungal-Bacterial Cooccurrence Patterns Differ between Arbuscular Mycorrhizal Fungi and Nonmycorrhizal Fungi across Soil Niches. *mBio*, *12*(2), e03509-20. https://doi.org/10.1128/mBio.03509-20

Zhang, K., Dang, H., Zhang, Q., & Cheng, X. (2015). Soil carbon dynamics following land-use change varied with temperature and precipitation gradients: Evidence from stable isotopes. *Global Change Biology*, *21*(7), 2762–2772. https://doi.org/10.1111/gcb.12886

**Statements and Declarations:**

**Funding:**

This research was supported by the Department of Energy, Sigma Xi Grants in Aid of Research, the UC Natural Reserve System Mathias Grant, and a UC Merced Committee on Research Senate Award. This research was also supported by the U.S. Department of Energy, Office of Biological and Environmental Research, Genomic Science Program 'Microbes Persist' Scientific Focus Area (#SCW1632) at Lawrence Livermore National Laboratory (LLNL).

**Competing Interests:**

All authors declare they have no competing financial interests.

**Author Contributions:**

Material preparation, sample collection, data collection, and analysis were performed by Leila Wahab. The first draft of the manuscript was written by Leila Wahab, and all authors comments on previous versions of the manuscript. All authors read and approved the final manuscript.

**Data Availability**

All of the data used for this study, including meta data and soil elemental/isotopic data, is available in the Dryad Open data repository (preliminary link that is private until the manuscript is published: https://datadryad.org/stash/share/qWsU4uKfHSePzs54nP24rrUhRNbLCz0htfUPoRK9qd0)

## Figures

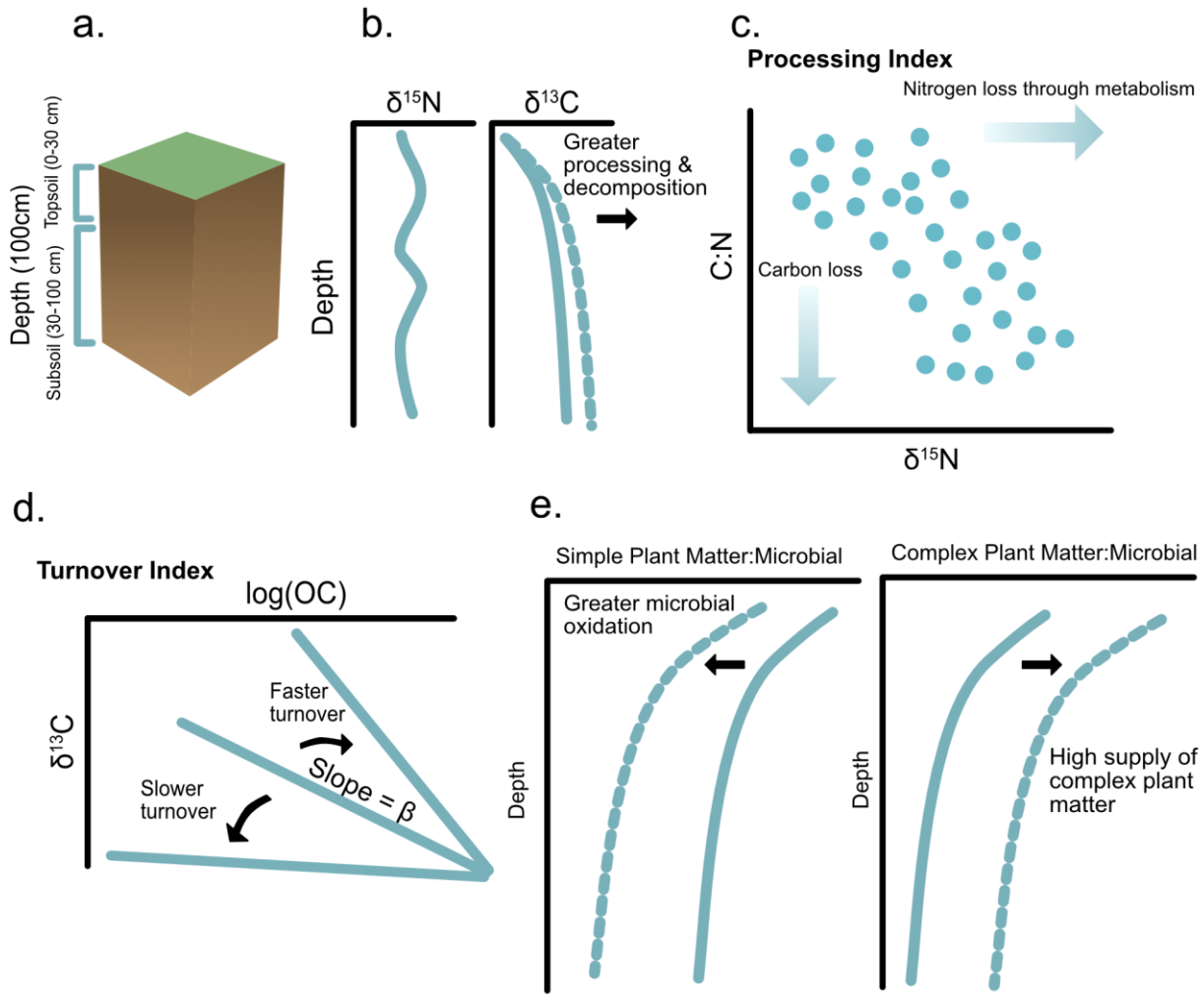


*Figure 1: Conceptual figure and overview of isotopic methodologies used in this study. Panel a indicates how we will define topsoil versus subsoil for our study, where topsoil refers to the top 30cm. Panels b-d show the isotopic methodologies used in this study. Panel b shows depth profiles of stable isotope values, and our stable isotope measurements of interest ($\delta^{13}C$ and $\delta^{15}N$). Panel c shows an isotopic proxy we used for processing, termed our processing index, the relationship between $\delta^{15}N$ and C:N. Panel d shows an isotopic proxy we used for turnover, beta, which is defined as the slope derived from relationship between the log transformed organic C and $\delta^{13}C$ values.*

*Table 1: Description of study sites. Temperature and precipitation data was sourced from California Irrigation Management Information systems (CIMIS) for Hopland and Sedgwick and Dendra (a cyber-infrastructure project for real time data storage) for Angelo. Mean annual precipitation and mean annual temperature data from 2012-2022 are reported. Temperature max/min refer to the mean maximum and minimum temperatures at each site. pH and textural information sourced from Foley et al. 2023 and are only measured for soils from 0-10cm. NDVI was collected from MODIS data from 2020 and represents an annual average as proxy of plant inputs at each site.*

| | **Angelo** | **Hopland** | **Sedgwick** |
|---|---|---|---|
| **MAP (mm/year)** | 126 | 58 | 24 |
| **MAT (C°)** | 11.7 ± 1.6 | 14.1 ± 1.6 | 14.6 ± 0.07 |
| **Temp Max/Min (C°)** | 20.4/4.6 | 22.0/9.0 | 19.7/9.0 |
| **Location coordinates** | 39° 44' 20.58" N | 39° 0' 1.6128" N | 34° 42' 43.8876" N |
| | -123° 37' 51.4956" W | -123° 5' 30.6276" W | -120° 2' 21.3936" W |
| **Elevation (m)** | 475 | 180 | 260 |
| **Soil Order** | Alfisol | Mollisol | Mollisol |
| **Soil Taxonomy** | Ultic Haploxeralfs | Typic Argixerolls | Pachic Haploxerolls |
| **pH** | 5.02 | 5.55 | 6.99 |
| **Sand/silt/clay (%)** | 28/42/27 | 45/36/19 | 38/28/34 |
| **NDVI** | 0.87 | 0.48 | 0.43 |

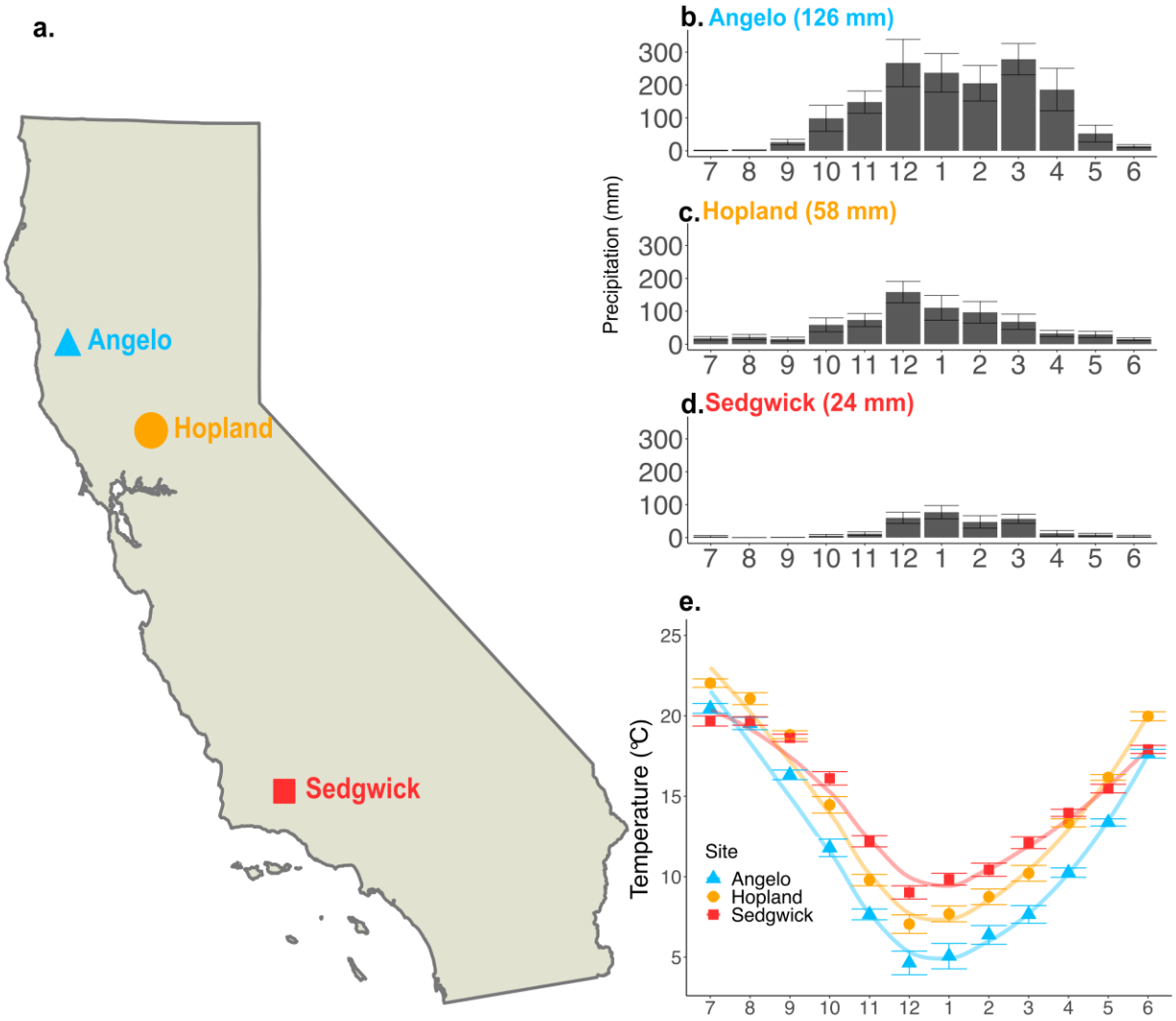


*Figure 2: Map of three Mediterranean climate California annual grassland sites sampled for this study. (a) Geographic location of sites in California. (b-d) shows average monthly precipitation in mm from 2012-2022, with Mean Annual Precipitation over the same period indicated in parentheses by the label. Data was sourced from California Irrigation Management Information systems (CIMIS) for Hopland and Sedgwick and Dendra (a cyber-infrastructure project for real time data storage) for Angelo. Months are numbered, and plots start in July to center the wet season. (e) Average monthly temperatures for each site from 2012-2022.*

*Table 2: Functional group assignments for the bands of interest used to evaluate DRIFT spectra. Based on Mainka et al. 2022*

| Functional Group | SOM type | Wavenumber center (range) $cm^{-1}$ |
|---|---|---|
| Aliphatic C-H stretch | Simple Plant Matter | 2925 (2976-2998) |
| | | 2850 (2870-2839) |
| Aromatic C=C stretch | Complex Plant Matter | 1525 (1550-1500) |
| Amide, quinone, ketone C=O stretch, aromatic C=C, and/or carboxylate C-O stretch | Microbially associated OM | 1620 (1660-1580) |

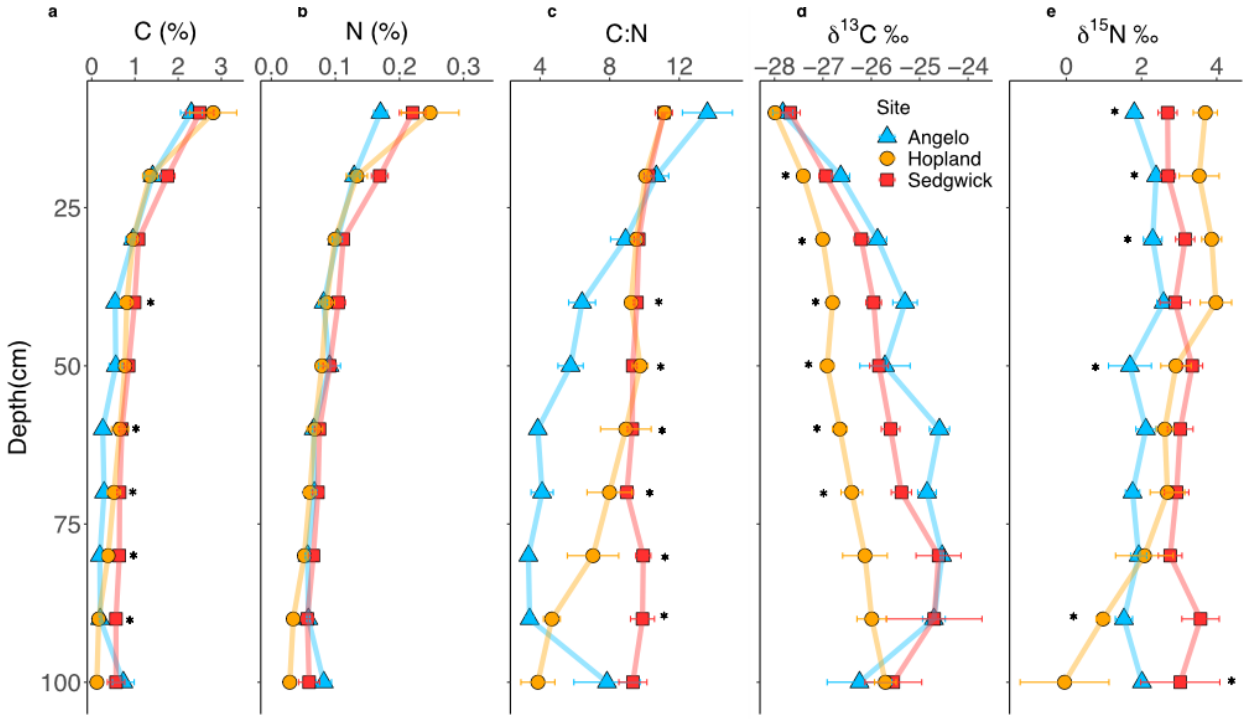


*Figure 3a-e: Elemental and isotopic variations in soils collected with depth across a precipitation gradient of three CA annual grasslands (from wetter to drier, Angelo>Hopland>Sedgwick). Plots show averages with standard error calculated for each 10 cm depth interval (n=7 for Hopland and Sedgwick, n=4 for Angelo). Stars indicate significant differences (p<0.05) according to one-way ANOVA by depth interval*

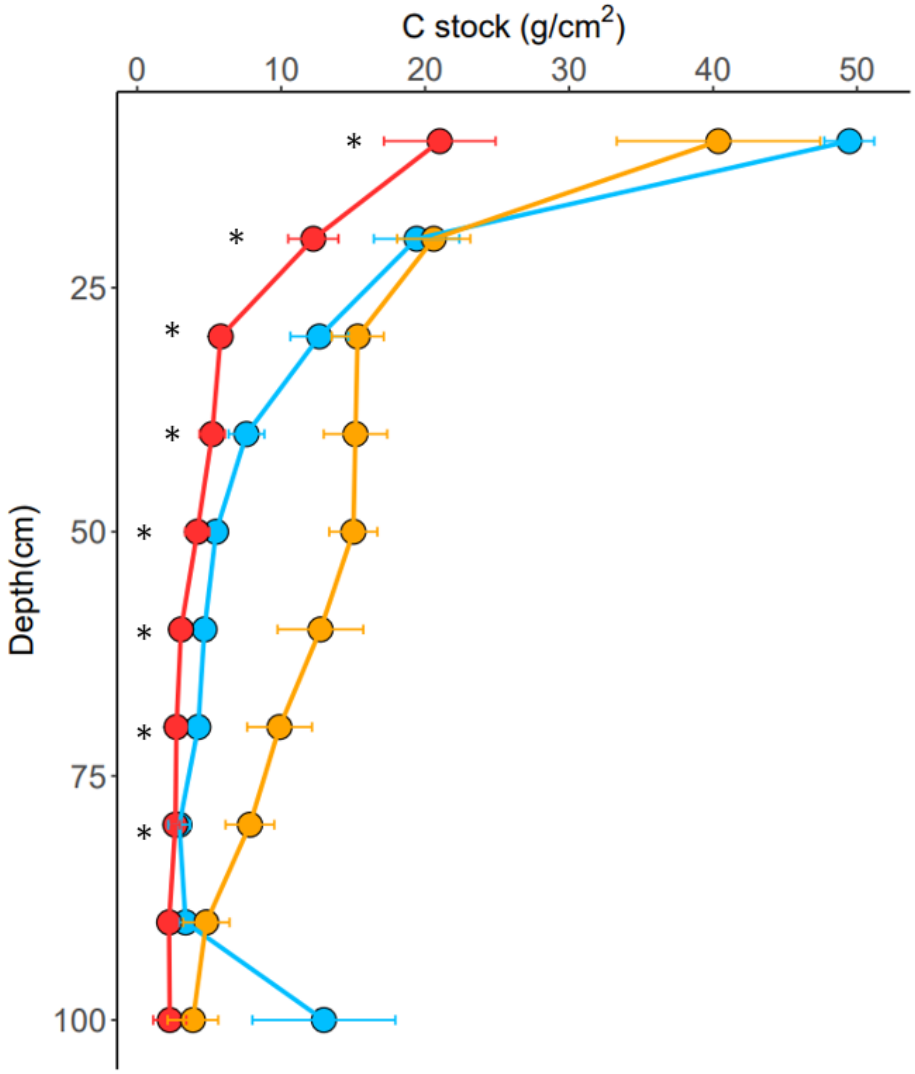


*Figure 4: Carbon stock data in soils collected with depth across a precipitation gradient of three CA annual grasslands (from wetter to drier, Angelo>Hopland>Sedgwick). Plots show averages with standard error calculated for each 10 cm depth interval (n=3 for Hopland and n=4 for Angelo). Stars indicate significant differences ($p<0.05$) according to one-way ANOVA by depth interval. Carbon stocks at Angelo and Hopland were calculated based on geoprobe cores, whereas data at Sedgwick was calculated through a pedo-transfer function.*

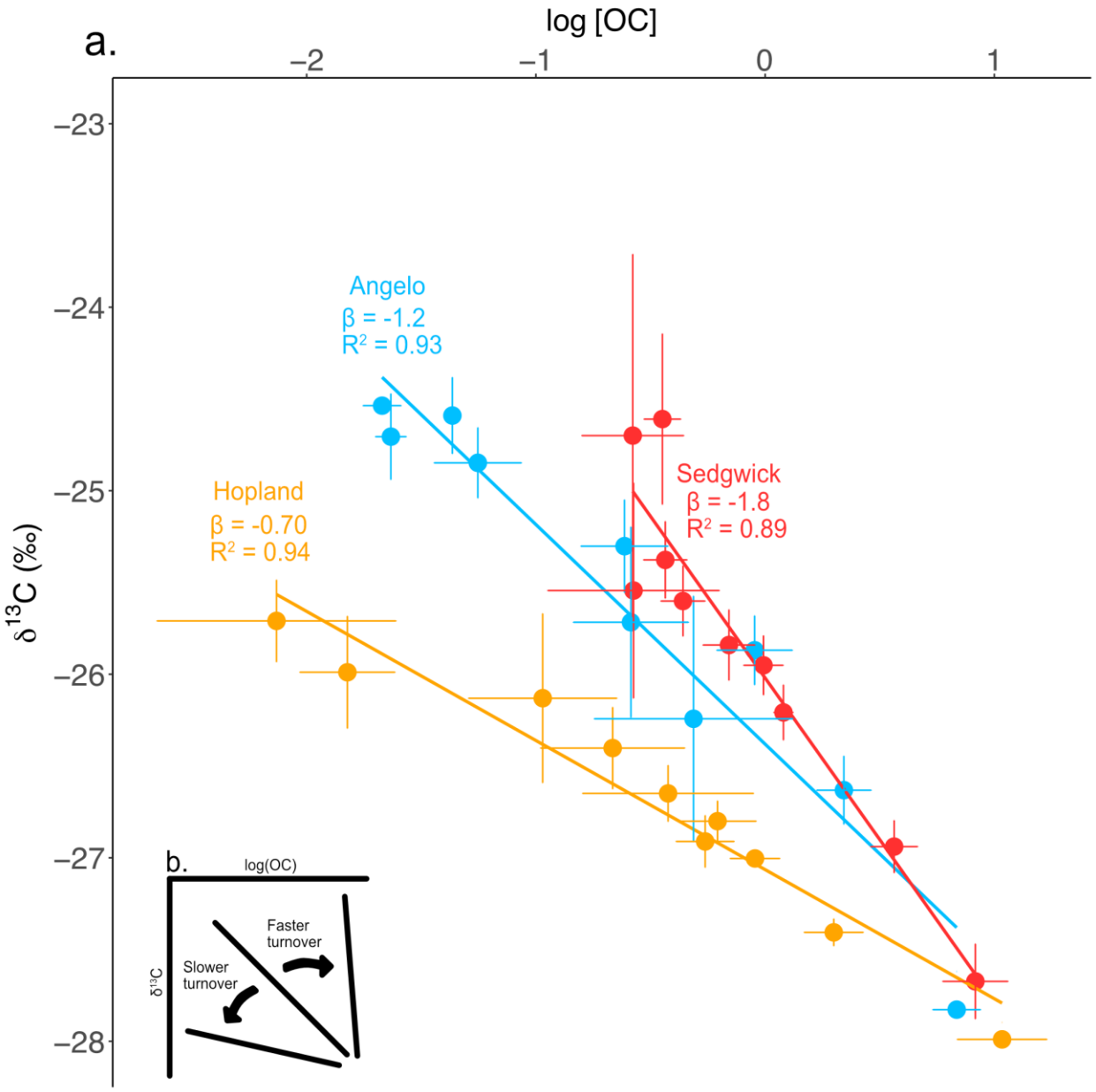


961
962
963

*Figure 5a-b: (a) variations in soil β values for three CA annual grasslands across a precipitation gradient. $R^2$ is the coefficient of determination for each regression line. (b) is a conceptual diagram for interpretations of beta. Beta values represent the slope between the log of organic carbon and $\delta^{13}C$ values, thought to be indicative of turnover time of soil (Brunn et al. 2016) (n=7 for Hopland and Sedgwick, n=4 for Angelo). We interpreted beta as our turnover index.*

964
965
966
967
968

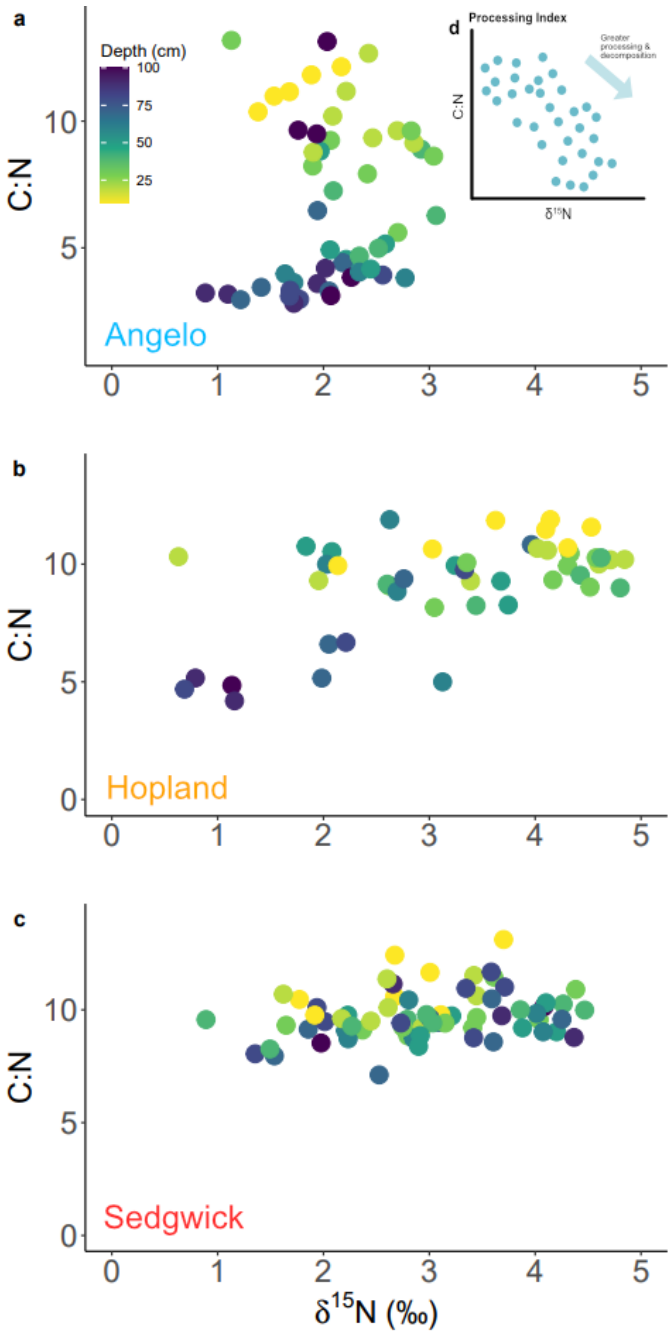


*Figure 6a-d: C:N versus $\delta^{15}N$ values for each site. All samples are plotted, and color scale indicates depth of sample (lighter = shallower, darker = deeper).We interpreted the distribution of C:N vs $\delta^{15}N$ as our stability index, and plotted these for a) Angelo, b) Hopland, and c) Hopland. Part d is a conceptual diagram indicating an interpretation for the relationship between C:N and $\delta^{15}N$ values.*

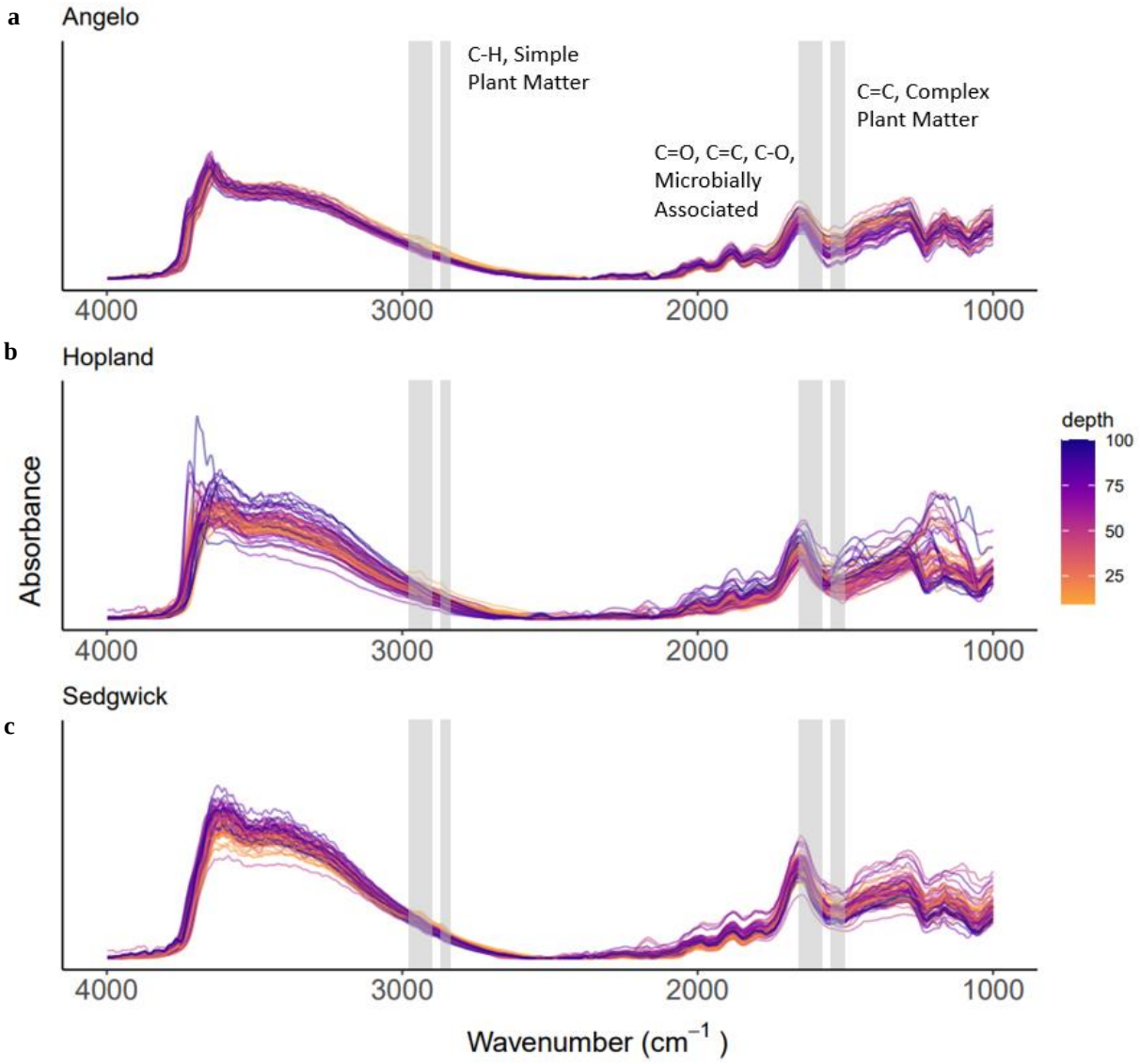


*Figure 7(a-c): DRIFTS spectra across sites and depths labelled with wavenumbers of interest. 2976-2998 cm$^{-1}$ and 2870-2839 cm$^{-1}$ represent aliphatic compounds and simple plant matter. 1550-1500 cm$^{-1}$ represents aromatic compounds and complex plant matter. Finally, 1660-1580 cm$^{-1}$ represents amide, quinone, ketone stretch, aromatic and/or carboxylate stretch, and microbially associated OM.*

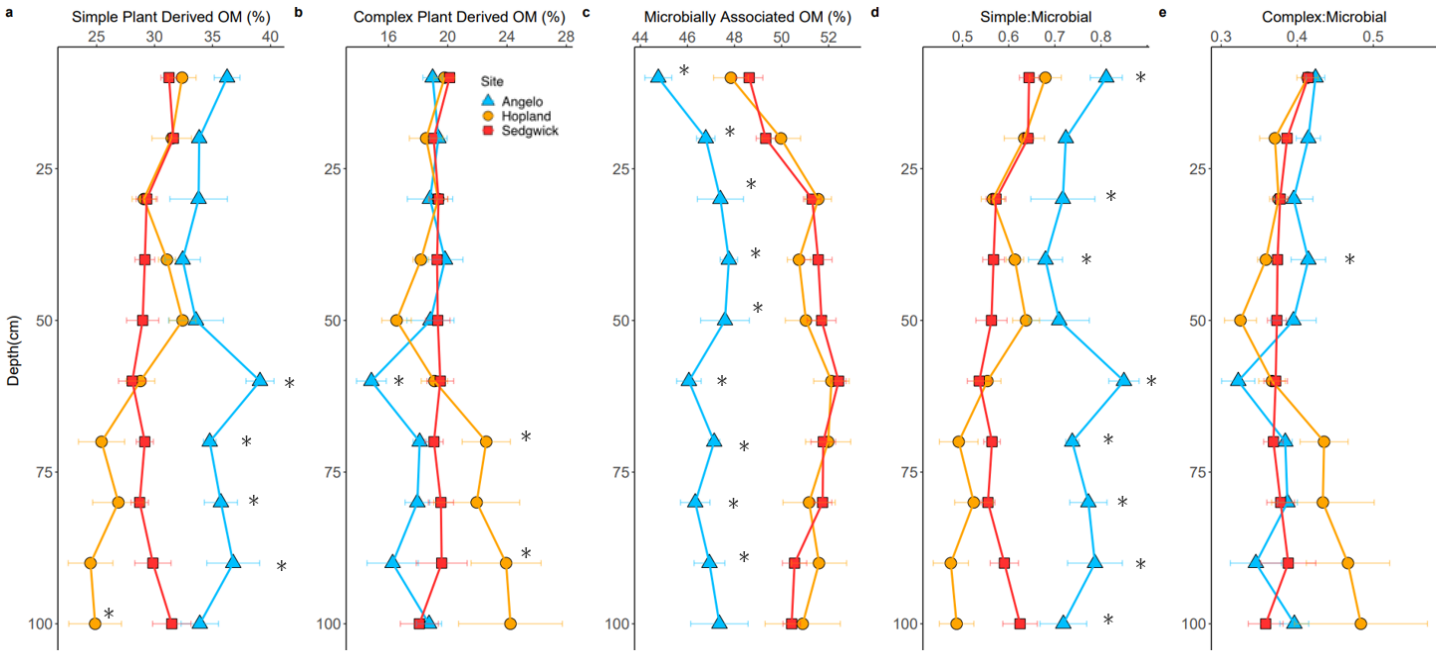


*Figure 8a-e: Proportions of integrated area for areas of interest in DRIFTS data. Panel a show the proportion of simple plant derived functional groups (2976-2998 $cm^{-1}$ and 2870-2839 $cm^{-1}$), panel b shows the proportion of complex plant derived functional groups (1550-1500 $cm^{-1}$), and panel c shows the proportion of microbially associated OM (1660-1580 $cm^{-}$) for each site. Panels d and e show ratios of simple plant matter to microbial plant matter, and complex plant matter to microbial plant matter respectively. Plots show averages with standard error calculated for each 10 cm depth interval (n=7 for Hopland and Sedgwick, n=4 for Angelo). Stars indicate significant differences ($p<0.05$) according to one-way ANOVA by 10cm depth interval.*